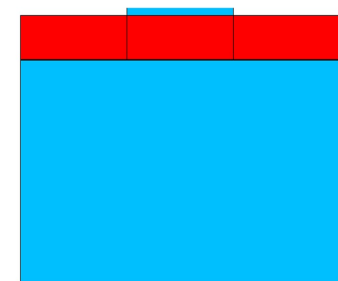
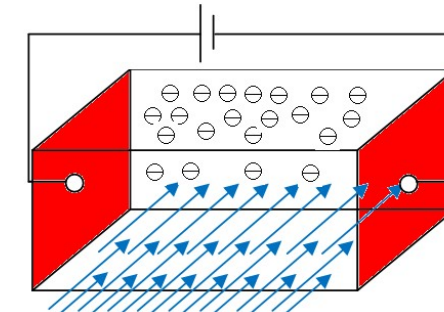
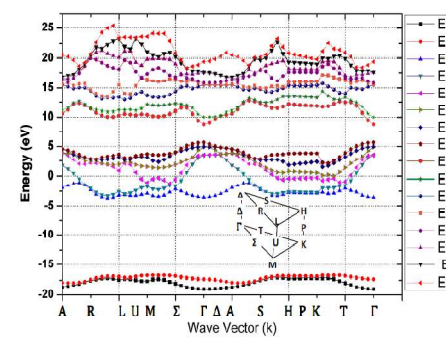
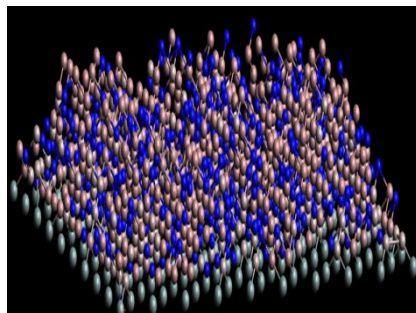




# Hot Carrier Dynamics: THz Spectroscopy Characterization



*Technology of Next Level  
driven through innovation*



# THz PULSES: Hot CARRIER TRANSPORT



- TNL-TS (THz Spectroscopy) simulator: an innovative technique applied for accurate predictions about hot carrier transportation properties.
- Capable to simulate the free particle motion on the three valleys over full band structure refer to as the free flight of the carrier and terminated by instantaneous random scattering events.
- Solution of BTE through Monte Carlo (MC) method: generating random free flight times for each particle, choosing the types of scattering processes based on specific material.
- Scattering events change the final energy and momentum of the particle after the scattering mechanism,
- Repeating the same procedure for the next free flight.



# Full Band Structure Analysis



# FULL BAND STRUCTURE



- The non-equilibrium time evolution of carriers and low-energy excitations within *sub-picoseconds (ps) time resolution* due to the interaction with the THz photons involves several additional complications.
- The formulation of charge carrier dynamics on the electronic band structure is *beyond the equilibrium transport conditions*.
- The structure and size of material itself dictate and decide the physics of the collision processes due to the presence of localized phonons, interfacial excitations etc.



# MATERIAL ENGINEERING



Electronic band structure calculation → Two general categories

## *Ab-initio* methods

- Hartree-Fock or Density Functional Theory (DFT),
- Utilize a variational approach to calculate the ground state energy of a many-body system
- Computationally very expensive, sometimes require massively parallel computers

## Empirical methods

- Orthogonalized Plane Wave (OPW)
- Tight-binding [the Linear Combination of Atomic Orbitals (LCAO) method]
- the local empirical pseudopotential method (EPM)
- the non-local empirical pseudopotential method (EPM).

**Empirical methods: computationally less expensive a relatively easy for generating electronic band structure with accuracy.**

# MATERIAL CHARACTERIZATION



*Plane waves and empirical pseudopotentials*: proven useful technique to gain insight into the electronic excitation spectrum of the solids The electron wave function is the solution to the time-independent Schrödinger equation:

$$\left( \frac{\hbar^2}{2m} \nabla^2 + E \right) \phi(r) = 0$$

□ The solutions form the basis of plane waves:

$$\phi_k(r) = C_k e^{ik \cdot r}$$

with

$$k^2 = k_x^2 + k_y^2 + k_z^2 = \frac{2mE}{\hbar^2}$$



# MATERIAL PARAMETERS EXTRACTION



The velocity,  $v$ , of a particle represented by a wave packet centered around the crystal momentum,  $k$ , is obtained from the *dispersion relation between  $k$  and the energy  $E$  as*

$$E_k = \frac{\hbar^2 k^2}{2m} \dots \dots \dots v = < \left| \frac{\hbar}{i} \nabla \right| > = \frac{1}{\hbar} \nabla_k E_k = \frac{\hbar k}{m}$$

**Density of States:**

$$D(E)dE = \frac{2m^{3/2} E^{1/2}}{\sqrt{2\pi^3 \hbar^3}} dE$$

**Effective Mass:**

$$m^* = \hbar^2 \left[ \frac{d^2 E}{dk^2} \right]^{-1}$$

**Energy Band gap:**

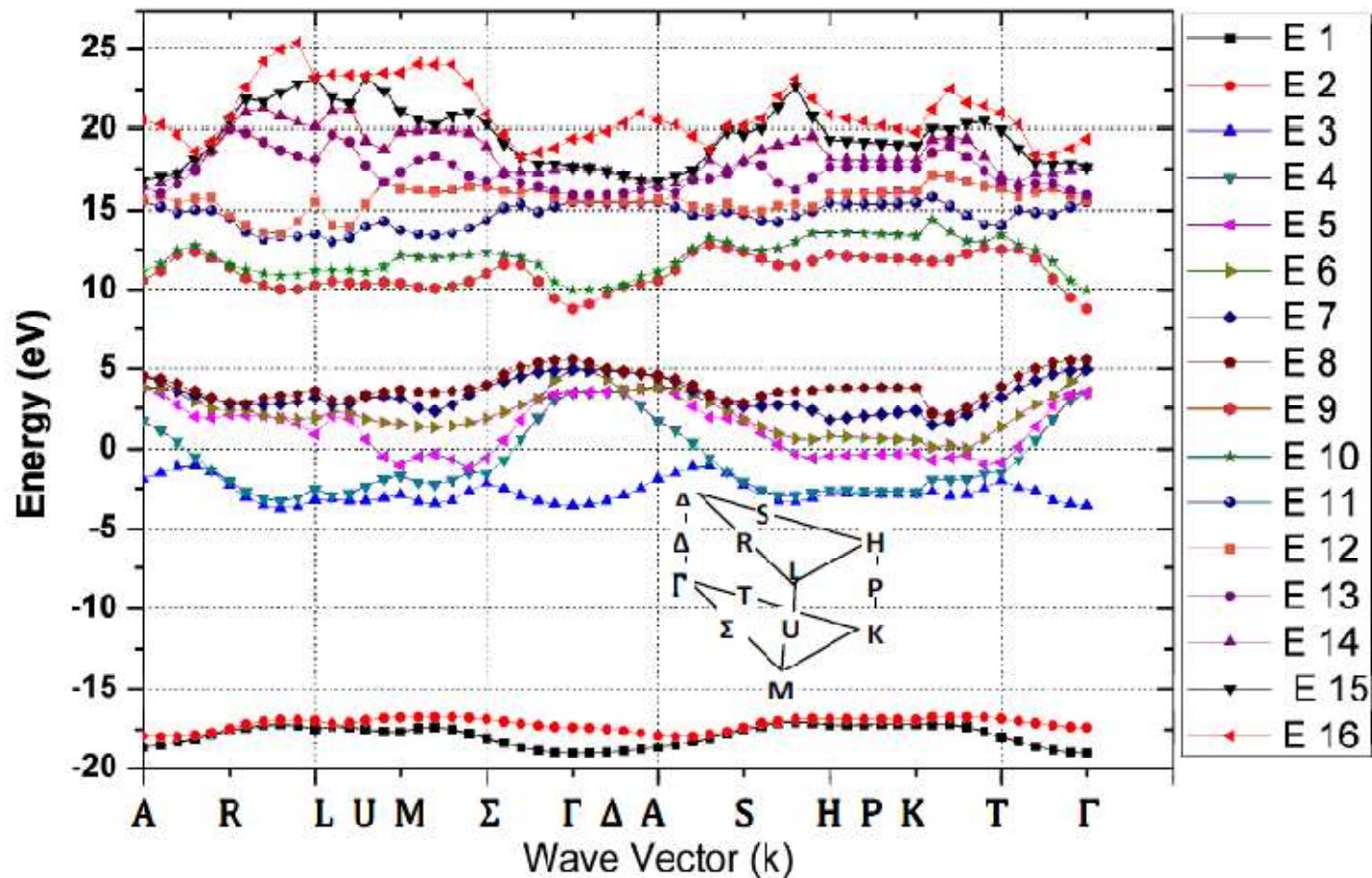
$$E_g = E_{D\text{Orbital}}^{\minima} - E_{\Gamma}^{\maxima}$$

D- orbital known as conduction energy levels for  $sp^3$  &  $sp^2$  hybridization materials

# TNL-FULL BAND SIMULATOR



- ❑ IV, III-V and II-VI alloys using ONLY lattice constant “a” of the compounds.
- ❑ Virtual Crystal approximation used to obtain “a” for ternary alloys.
- ❑ Inclusion of a semi-empirical disorder contribution.
- ❑ Non-Parabolicity & Parabolicity effects
- ❑ Various bands and valleys
- ❑ The absolute minima of the conduction band lie at the  $\Gamma$  point.
- ❑ Main valleys energies, effective masses with non-parabolicity factors, carrier group velocity, DOS etc.



# CASE STUDY: ZnO Thin Film



Different DFT based calculated energy band gap of ZnO materials, LDA and PBE functional, LDA + U functional, and hybrid functional (HSE06) along with the lattice parameters, structural internal parameters ( $u$ ) and disorder constants ( $P$ ). The calibrated energy gap of ZnO materials using TNL-FB simulator and Experimental band gap are also included for comparison.

DFT Methods	LDA	PBE	HSE06	LDA+U	Experimental	TNL-FB Simulator
$a$ (Å)	3.210 <sup>3</sup>	3.284 <sup>4,5</sup>	3.262 <sup>4,5</sup>	3.197 <sup>6</sup>	3.253 <sup>19-21</sup>	<b>3.254</b>
$c$ (Å)	5.136 <sup>3</sup>	5.296 <sup>4,5</sup>	5.212 <sup>4,5</sup>	5.154 <sup>6</sup>	5.205 <sup>19-21</sup>	<b>5.21</b>
$u$	0.380	0.378	0.381	0.378	0.380	<b>0.380</b>
$P^*$	0.000	0.002	-0.001	0.002	0.000	<b>0.000</b>
Eg (eV)	<b>0.7941<sup>3</sup></b>	<b>3.413<sup>4,5</sup></b>	<b>2.464<sup>4,5</sup></b>	<b>1.1541<sup>6</sup></b>	<b>3.44<sup>3-5</sup></b>	<b>3.428</b>

\* Journal of Electronic Materials , 2021.



# CASE STUDY: ZnO Thin Film



ZnO Samples	t <sub>DS</sub> (nm)			t <sub>WH</sub> (nm)	Strain	Lattice Constant		Internal Parameter u(P)	Bond Length (Å)	Optical Band gap (eV)	Simulated Band gap (eV)
	(100)	(002)	(101)			a (Å)	c (Å)				
Undoped	11	18	10	26	$6.5 \times 10^{-3}$	3.246	5.238	0.398	2.013	3.22	<b>3.22</b>
0.45at.% Cd	16	20	17	13	$-8.0 \times 10^{-3}$	3.328	5.190	0.4023	2.009	3.20	<b>3.19</b>
0.51at.% Cd	19	21	19	26	$1.5 \times 10^{-3}$	3.332	5.161	0.4025	2.007	3.19	<b>3.22</b>
0.56at.% Cd	11	18	10	31	$10.0 \times 10^{-3}$	3.313	5.225	0.4040	2.006	3.15	<b>3.15</b>
1at.% Sr	14	10	17	7.48	$-1.64 \times 10^{-2}$	3.256	5.194	0.389	1.978	3.25	<b>3.27</b>
2at.% Sr	21	9	16	10.27	$4.27 \times 10^{-2}$	3.251	5.194	0.389	1.976	3.26	<b>3.26</b>
3at.% Sr	9	6	6	4.14	$9.95 \times 10^{-2}$	3.271	5.223	0.389	1.988	3.28	<b>3.33</b>
1at.% Fe	5	8	9	1.43	$-14.8 \times 10^{-2}$	3.236	5.194	0.380	1.967	3.24	<b>3.26</b>
2at.% Fe	3	5	7	0.65	$-34.5 \times 10^{-2}$	3.231	5.194	0.380	1.968	3.26	<b>3.25</b>
3at.% Fe	8	5	7	9.06	$6.6 \times 10^{-2}$	3.231	5.186	0.380	1.970	3.29	<b>3.25</b>

Undoped, Cd, Sr and Fe doped ZnO thin films (Sol gel) along with optical and simulated energy band gaps

\* [Journal of Electronic Materials, 2021.](#)



# BAND GAP ENGINEERING



- The experimentally observed c/a ratios are found different compare to the ideal crystal.
- Strong correlation observed between the c/a ratio and the internal structure parameter (u)
- c/a ratio decreases, the u parameter increases in such a way that the four tetrahedral distances remain nearly constant through a distortion of tetrahedral angles due to long-range polar interactions

$$u = \frac{1}{3} \left( \frac{a}{c} \right)^2 + P + 0.25$$

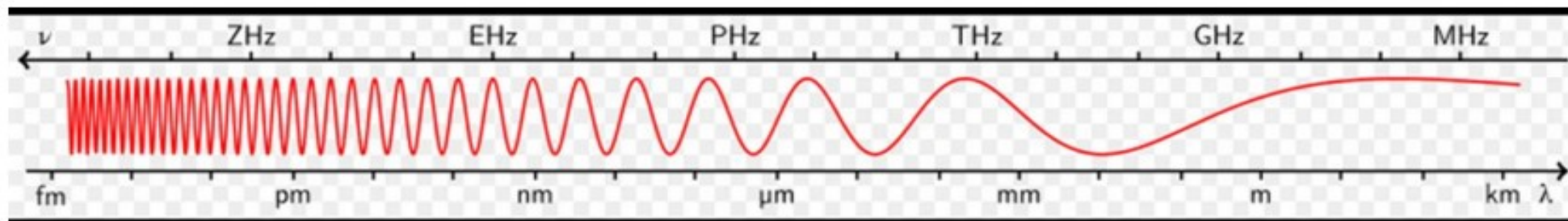
- The proposed model is verified against various experimental studies.
- The sol-gelgrown ZnO films have a different band structure and different band optical band gap due to inclusion of impurities
- Successfully explained the experimental results with disorder effects



# THz SPECTRUM



- **Terahertz waves are electromagnetic waves whose frequency range from 100 GHz to 10 THz, their wavelengths are between 30 μm and 3 mm.**



Technology	mmW	THz Band	Infrared	Visible Light Communication (VLC)	Ultra-Violet
Frequency Range	30 GHz - 300 GHz	100 GHz - 10 THz	10 THz - 430 THz	430 THz - 790 THz	790 THz - 30 PHz
Range	Short range	Short/Medium range	Short/Long range	Short range	Short range
Power Consumption	Medium	Medium	Relatively low	Relatively low	Expected to be low
Network Topology	Point to Multi-point	Point to Multi-point	Point to Point	Point to Point	Point to Multi-point
Noise Source	Thermal noise	Thermal noise	Sun/Ambient Light	Sun/Ambient Light	Sun/Ambient Light
Weather Conditions	Robust	Robust	Sensitive	—	Sensitive
Security	Medium	High	High	High	To be determined

4

Source : research paper [EHA,18]



# ISSUES & CONCERNS



- Over the past decade the Drude-Smith model used successful in reproducing the localization signatures observed in a wide variety of materials

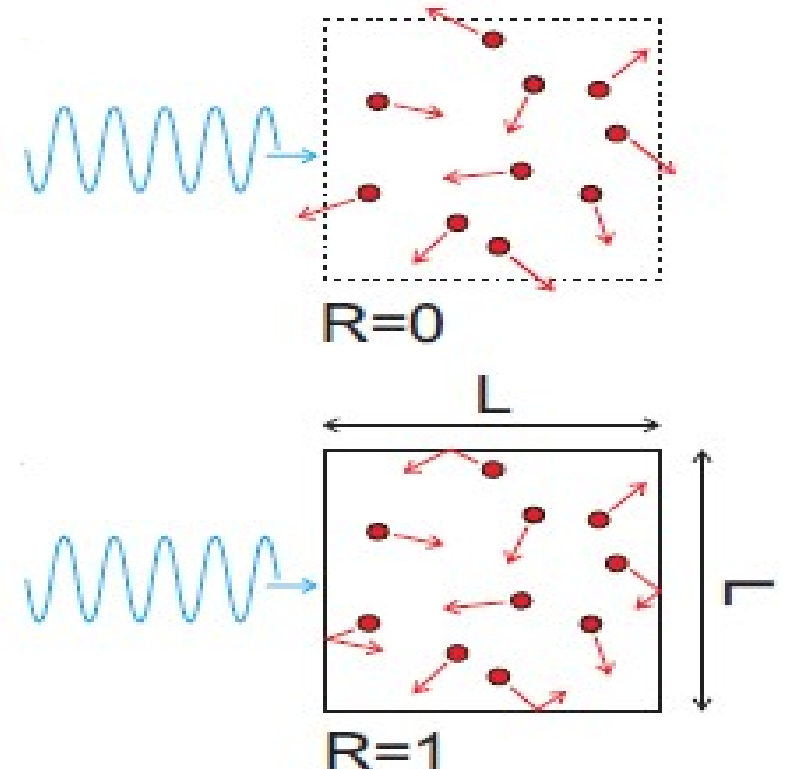
$$\tilde{\sigma}(\omega) = \frac{Ne^2\tau_{DS}/m^*}{1 - i\omega\tau_{DS}} \left[ 1 + \frac{c}{1 - i\omega\tau_{DS}} \right] \text{ with } c \text{ as localization (fitting) parameter}$$

- Strong deviations the Drude model even at mesoscopic scale (the size of the confining structure is comparable to the carrier mean free path)
- the Drude-Smith model bears two primary criticisms:
  - (i) No rigorous explanation for the assumption for backscattering
  - (ii) Fit parameters unknown beyond phenomenological expressions depend on multiple parameters
  - (iii) Low-frequency conductivity suppression in some nanomaterials

# Solutions: TNL-TS Simulator



- Monte Carlo technique for solution of BTE for hot carrier transport behavior
- Distribution function, carrier mobility, electron mean energy, population ratio, average drift velocity, conductivity and absorption as a function of THz frequency
- Dynamics of hot carriers with excitation and de-excitation
- Impact of various types of scatterings



# METHODOLOGY



$$\frac{df}{dt} + \mathbf{v} \cdot \nabla_{\mathbf{r}} f + \mathbf{F} \cdot \nabla_{\mathbf{p}} f = \frac{\partial f}{\partial t} \Big|_{\text{collision}}$$

Here  $f$  is the distribution function,  $\mathbf{F}$  is the FORCE field.,

$$\mathbf{F} = q\mathbf{E} = \frac{dp}{dt} = \hbar \frac{d\mathbf{k}}{dt}$$

$E$  is the THz field strength and  $\mathbf{k}$  is wave vector

- Solution of 6+1 dimensional is possible through:
  - Ensemble Monte Carlo (EMC) technique to simulate non-equilibrium transport in semiconductor physics is more straightforward and provides flexibility in exploring physical mechanisms and carrier transport.

# METHODOLOGY

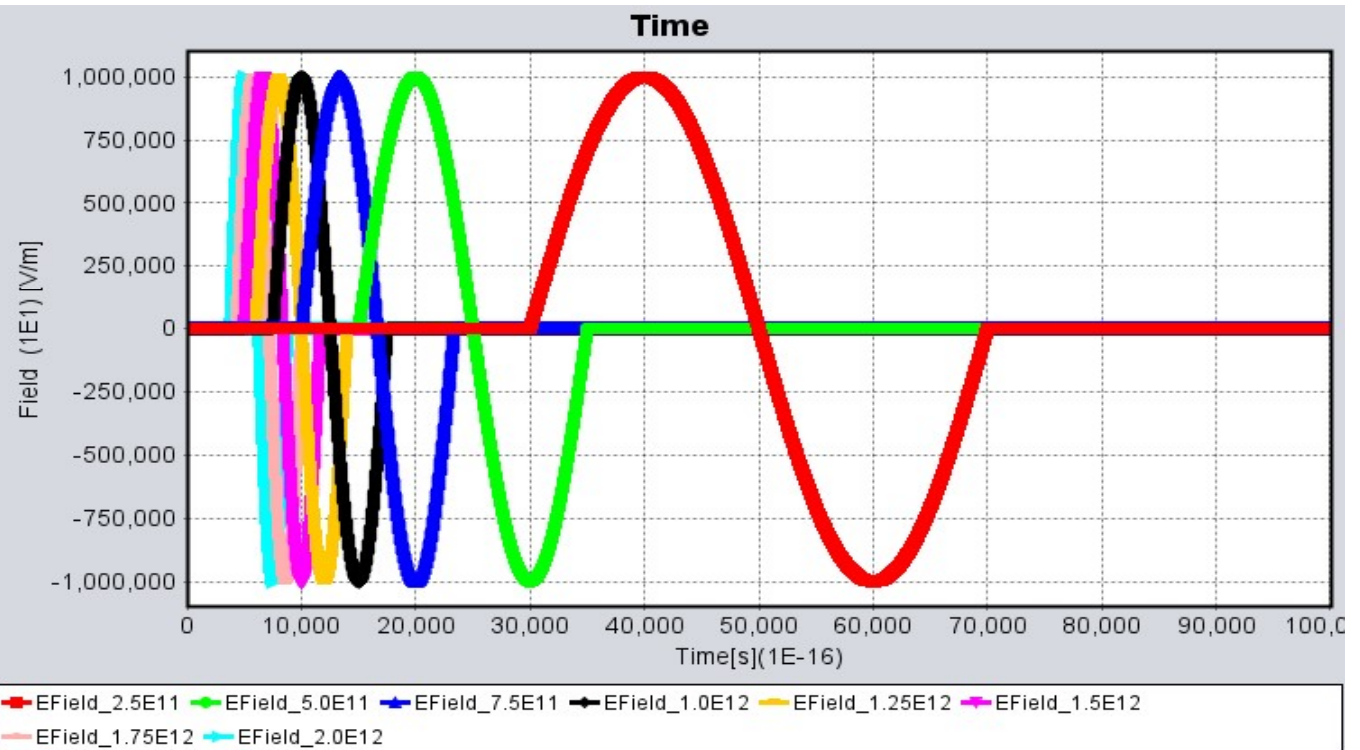


## □ Continuous THz Pulses

$$E = E_0 \cos(2\pi f n dt)$$

$E_0$  is the peak amplitude of the driving THz pulse,  $f$  is the THz pulse frequency,  $n$  is the number of total time steps and  $dt$  is the time step between two successive events (the duration of the carrier interaction)

- Total time scale for each THz pulse is 20ps, ensures one complete single cycle (period) of pulse.
- Condition  $f \geq 0.1 \text{ THz}$  during one complete iteration.



# METHODOLOGY



- Each particle's velocity in the y-direction at each time step

$$v_{y,n} = v_{y,n-1} + \frac{eE_0\Delta t}{m^*} \cos(2\pi f n \Delta t)$$

Here  $v_{y,n-1}$  is the y-component of the velocity at the previous time step, e is the elementary charge, and  $E_0$  is the amplitude of the driving field.

✓ Current Density (Time domain)

$$J(t) = Ne v_d(t) \alpha_n(E) L_{eff}$$

✓ Fourier Transformation

$$\sigma(\omega) = \frac{\sum J(t)(\cos \omega t + i \sin \omega t)}{\sum E(t)(\cos \omega t + i \sin \omega t)}$$

✓ Absorption Coefficient

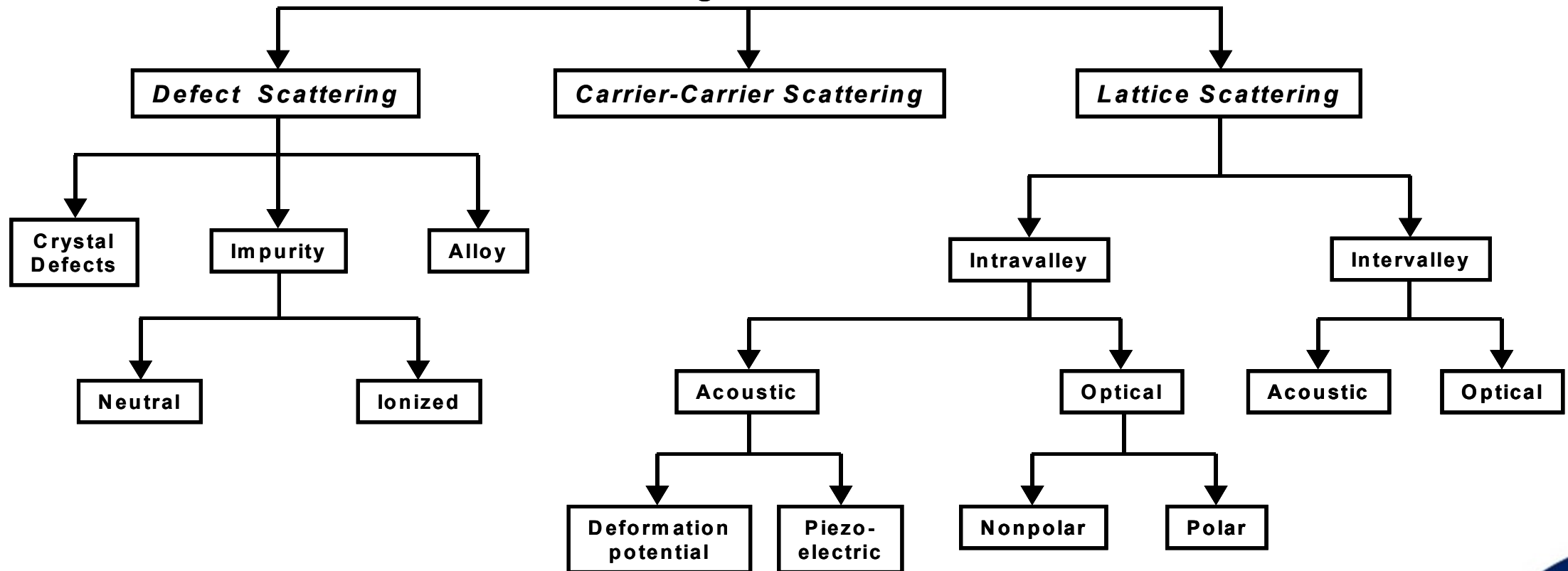
$$\alpha(\omega) = \frac{4\pi\sigma_R(\omega)}{n_r c}$$



# SCATTERINGS



## Scattering Mechanisms



# WORKING PRINCIPLE



- The first task is to generate free flights of random time duration for each particle.
- This time duration is governed by total time of Monte-Carlo simulation of 20ps divided in time steps  $dt$  of 0.4fs giving  $N=50000$  steps as a simulation points.
- The pulse is delayed by the time instant of  $\frac{3}{4}$ th of the time period of the applied THz signal.
- Assuming these condition one respective simulation will be run for 50000 steps over a period of 20ps.
- Hence, at least one period of the driving frequency is contained in every simulation wherein  $f \geq 0.1\text{THz}$ .
- By default 20000 particles are to be used.
- Flexibility to users: Number of Particles



# Case Studies: Ge



## Symmetry points

At k=0 showing L valley

$$L = \frac{2\pi}{a} \left( \frac{1}{2}, \frac{1}{2}, \frac{1}{2} \right)$$

At k=10, the curve shows the Gamma valley

$$\Gamma = \frac{2\pi}{a} (0, 0, 0)$$

At k=20, the curve shows the X valley

$$X = \frac{2\pi}{a} (1, 0, 0)$$

At k=25, the curve shows the W valley

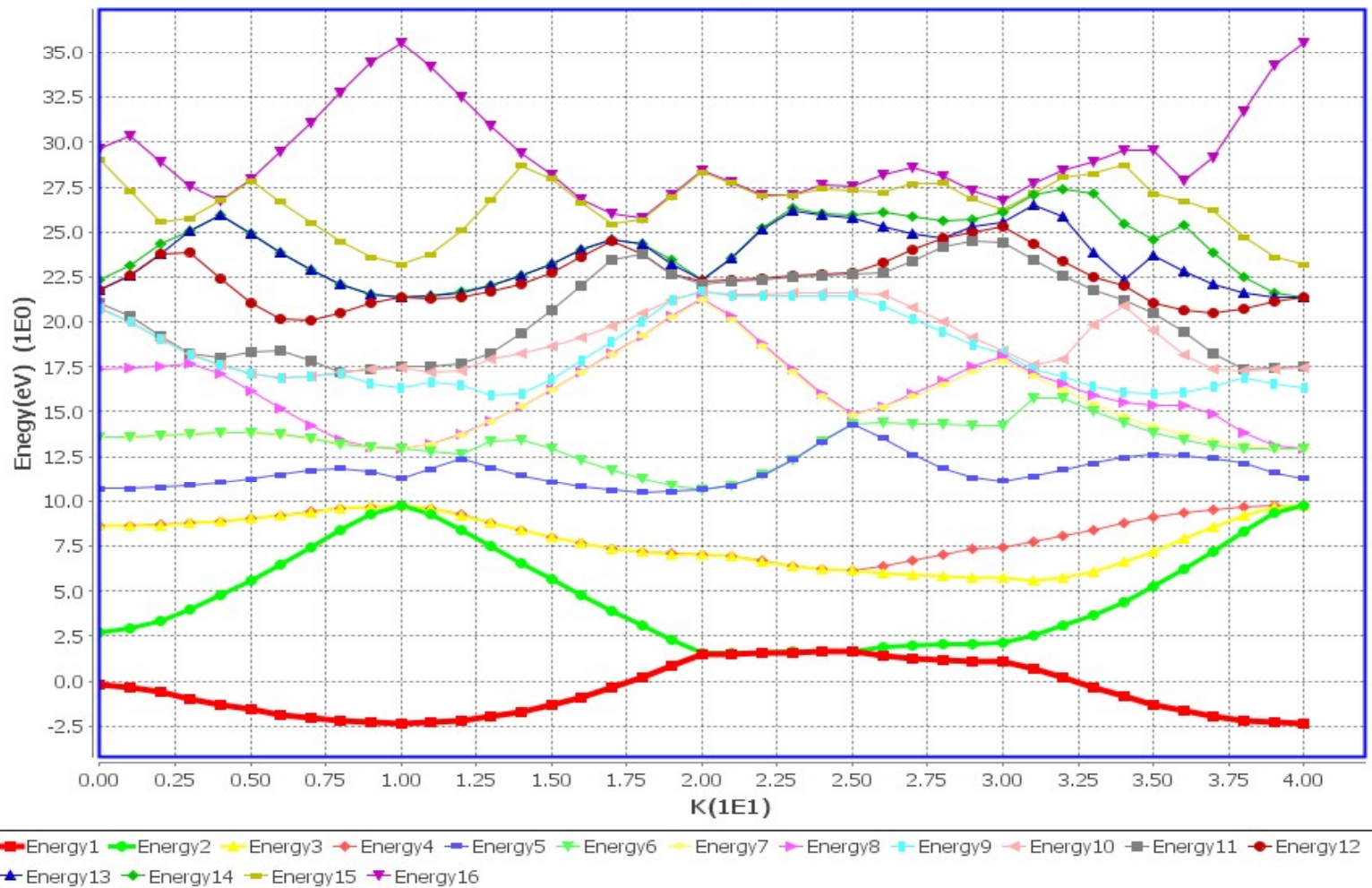
$$W = \frac{2\pi}{a} (1, \frac{1}{2}, 0)$$

At k=30, the curve shows the K valley

$$K = \frac{2\pi}{a} (\frac{3}{4}, \frac{3}{4}, 0)$$

At k=40, the curve again shows the Gamma valley

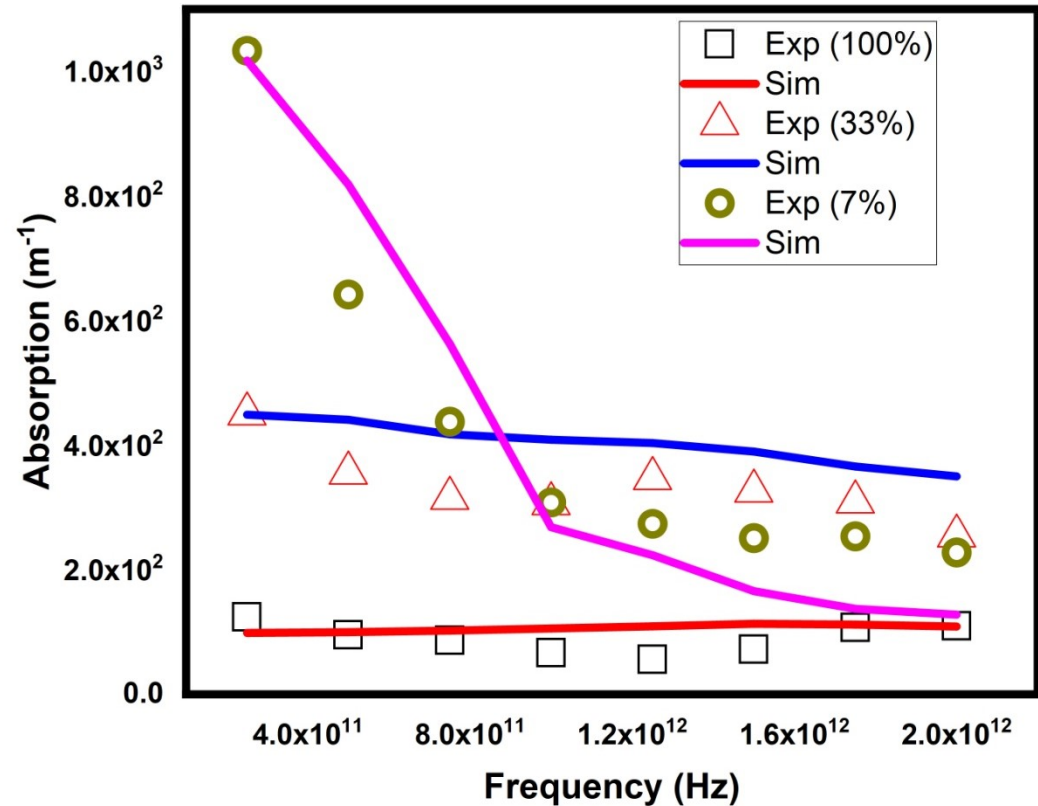
$$\Gamma = \frac{2\pi}{a} (0, 0, 0)$$



# Case Studies: Ge

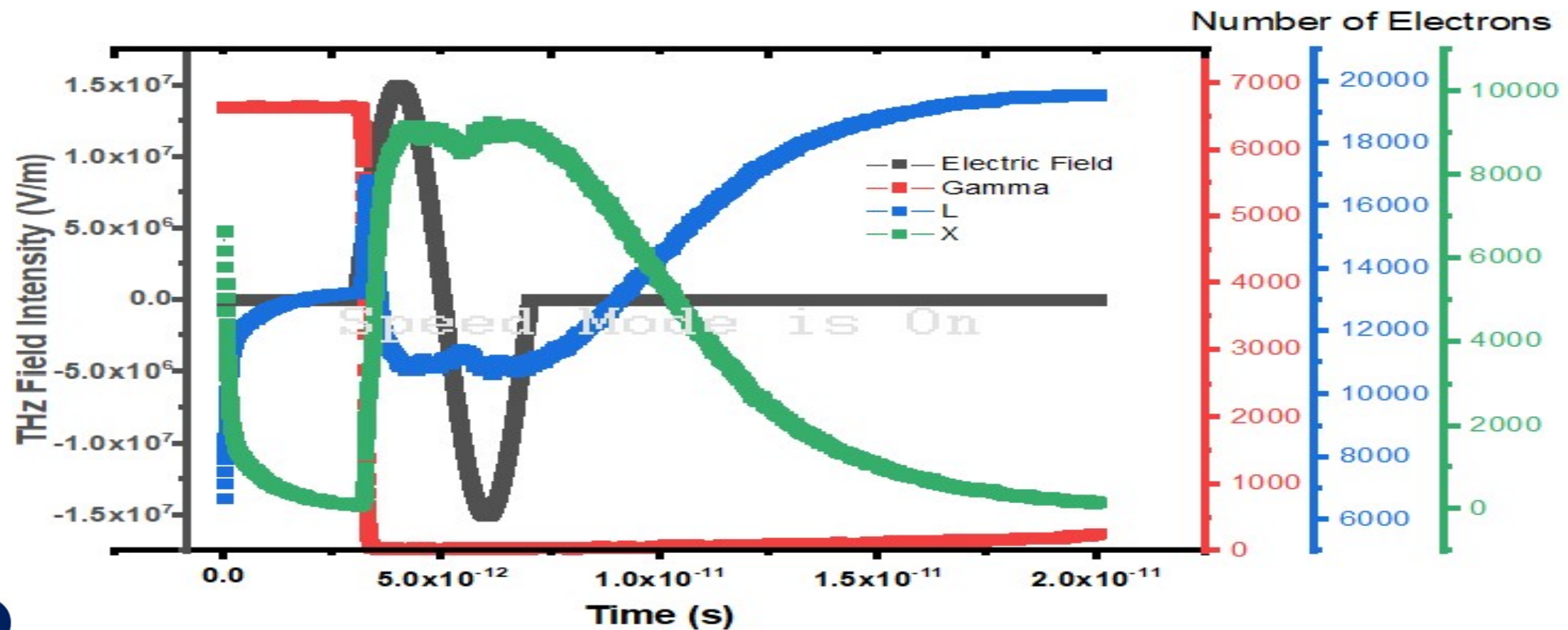


- Slight mismatch at field strengths  $5\text{MV/m}$  ( $0.8\text{ THz} - 1.2\text{ THz}$ ) and  $1\text{MV/m}$  ( $1.6\text{ THz} < f_{\text{THz}} < 2.0\text{ THz}$ ) respectively explained on the basis of the THz-induced Kerr effect (TKE),
- Change in refractive index exhibits quadratic dependence on an externally applied electric field .
- Experimental single-cycle THz pulses with  $\mu\text{J}$  energies is generated in a LiNbO<sub>3</sub> (LN) crystal by optical rectification of 100 fs pulses at 800 nm with the tilted-pulse-front method without explaining the scope of THz-induced Kerr effect which is dominant at low peak field strengths .



• János Hebling, Matthias C. Hoffmann, Harold Y. Hwang, Ka-Lo Yeh and Keith A. Nelson, Observation of non equilibrium carrier distribution in Ge, Si, and GaAs by terahertz pump-terahertz probe measurements, *Phys Rev B* 81, 035201 (2010).

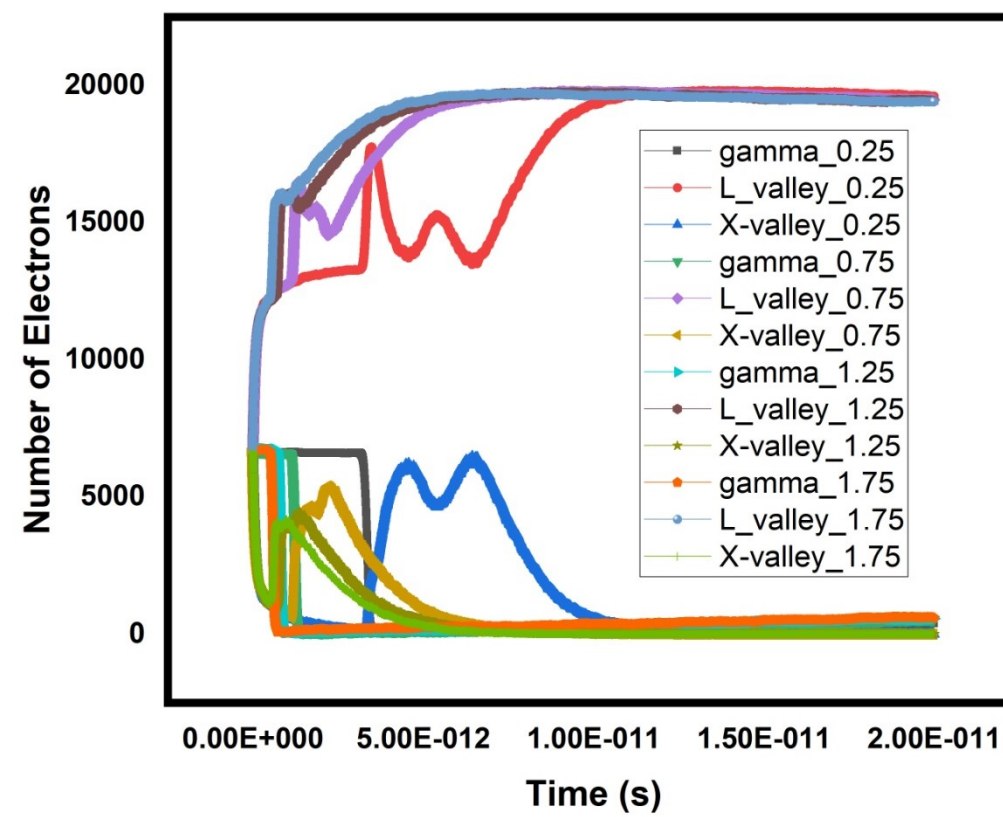
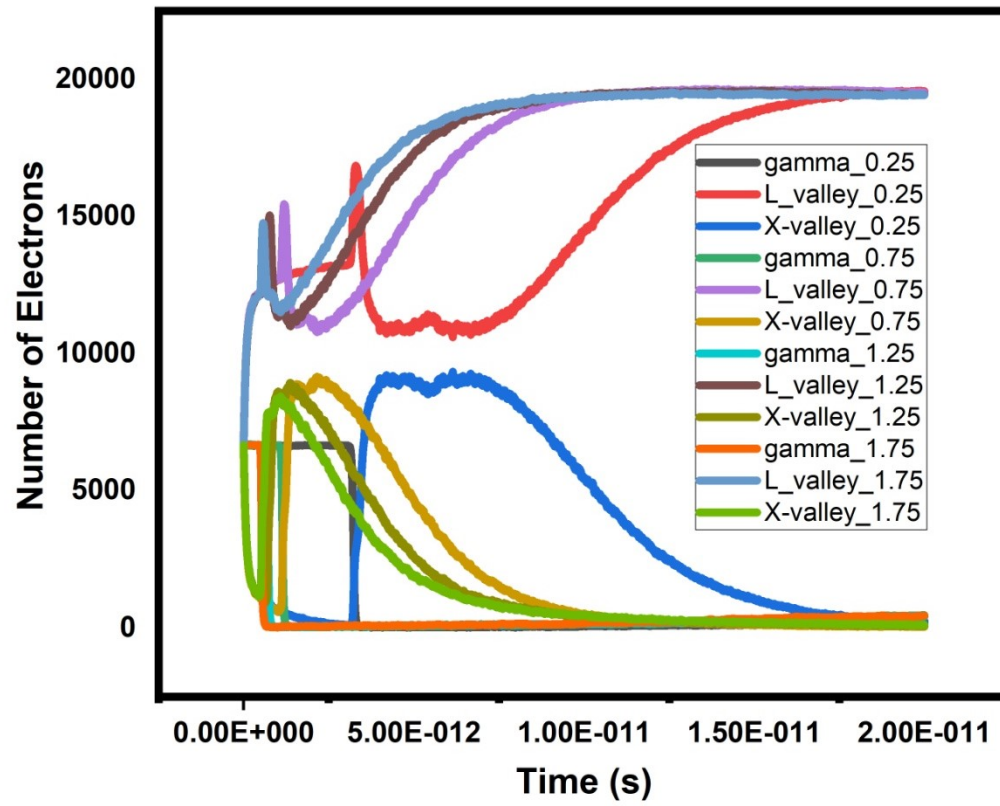
# Case Studies: Ge



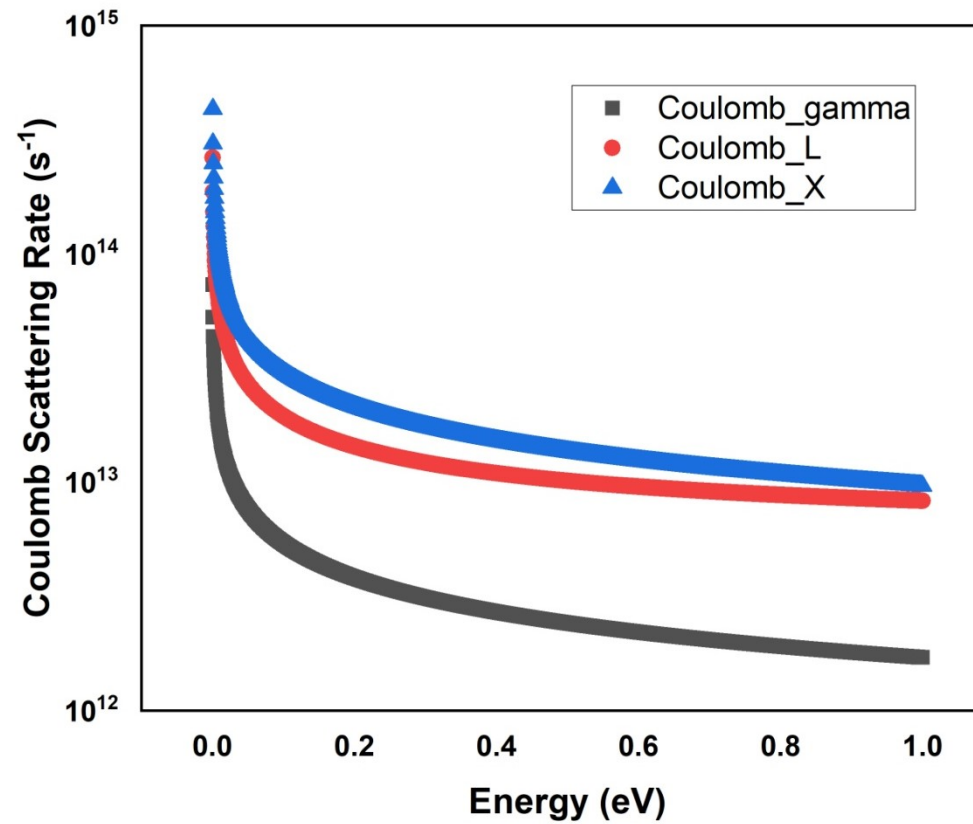
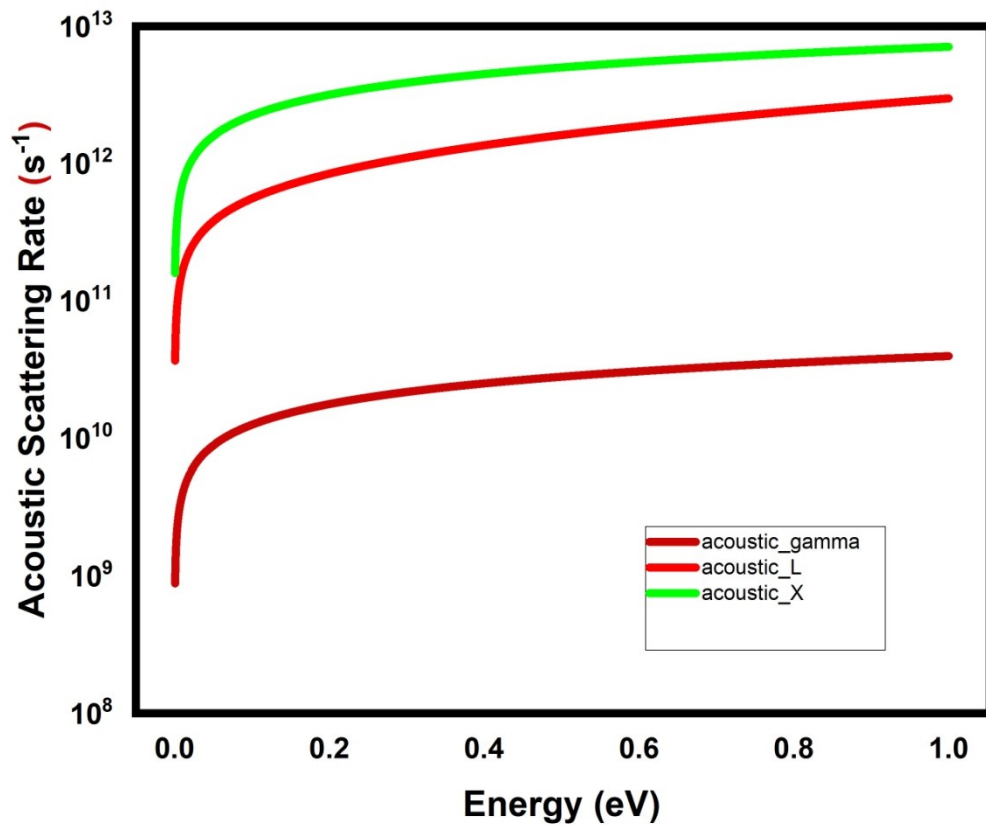
$\Gamma$  (Red), L(Blue) and X (Green) valleys with single cycle THz pulse (Black) with peak strength of 15 MV/m at 0.25 THz frequency



# Case Studies: Ge



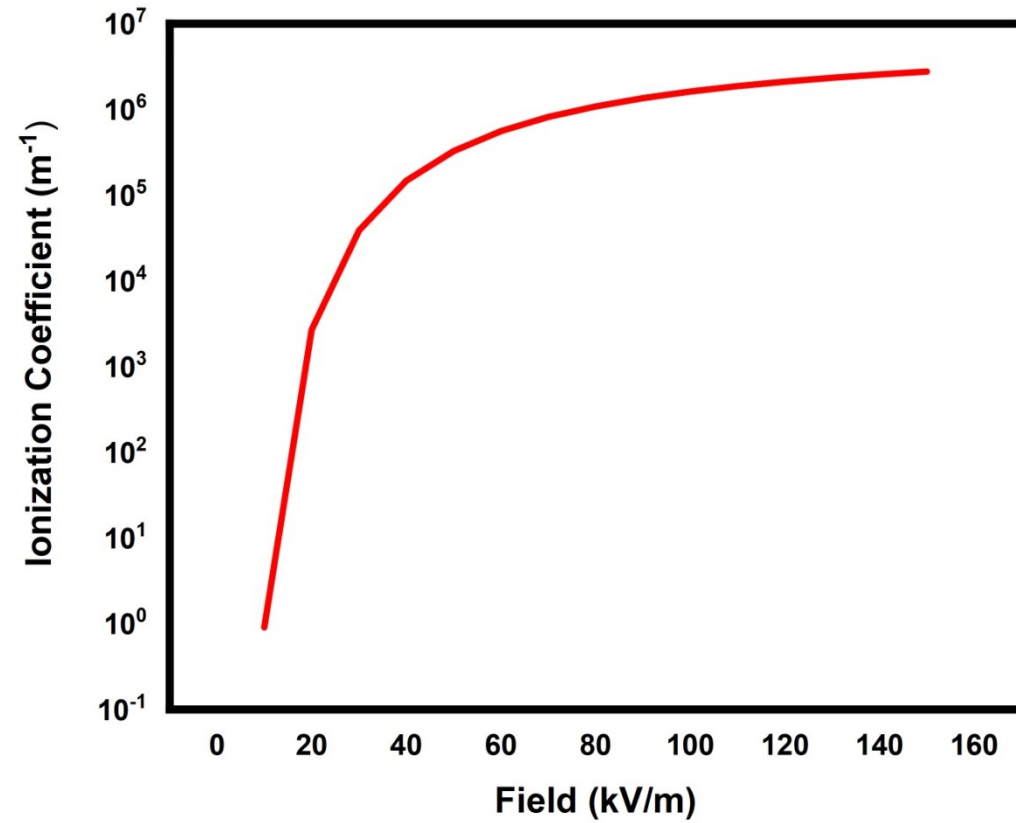
# Case Studies: Ge



# Case Studies: Ge



- The proper understanding of ultrafast nonlinear carriers dynamics on the basis of solid physical foundation is carried out.
- The significant contributions of the various types of scattering mechanisms on complex conductivity of Ge crystal have been observed.
- The experimental complex conductivity and free carrier absorption spectra are successfully demonstrated theoretically with the help of proposed atomistic technique.



# Case Studies: Ge



Experiments Calibrated  
for  
ELI-ALPS

ELI-HU Nonprofit Ltd., Dugonics tér 13. H-6720  
Szeged, Budapesti út 5, Hungary

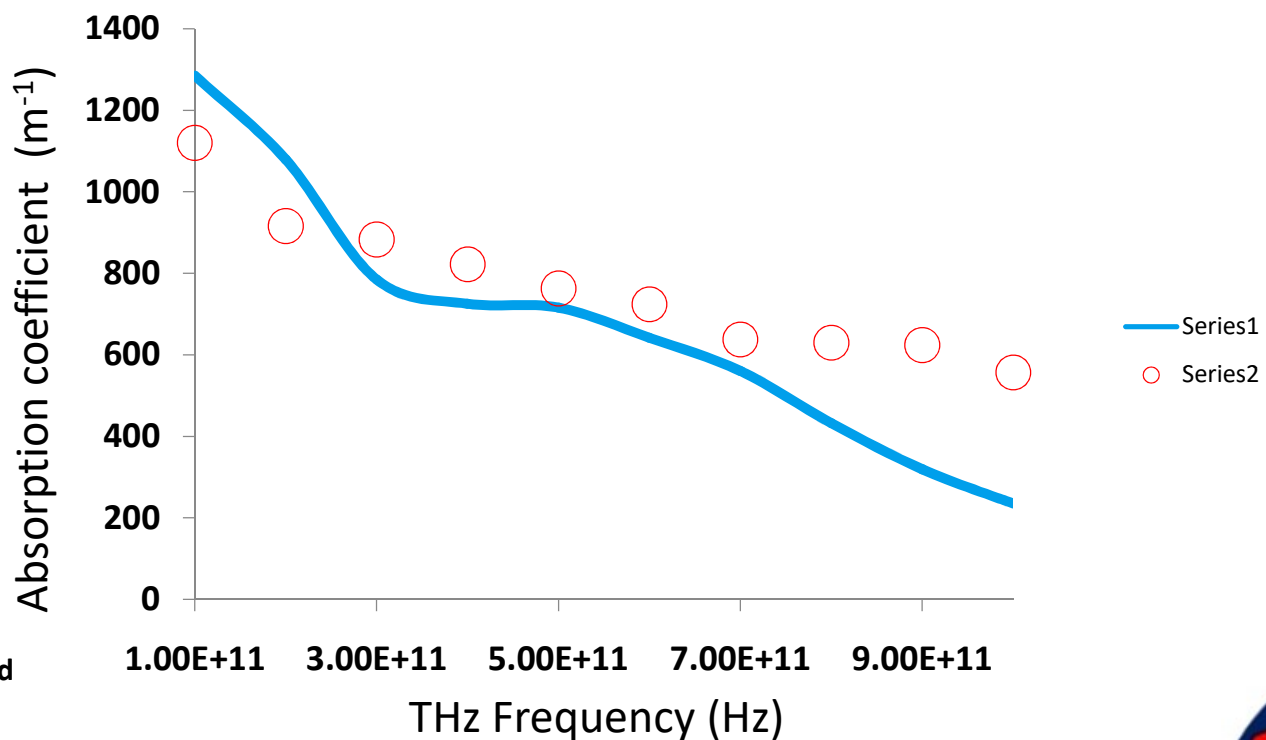
# Case Studies: Ge



## Absorption ( $\text{m}^{-1}$ ) with respect to THz Freq at 10 kV/cm

- Material: Ge “n doped”
- Temperature: 294 K
- Different THz fields
- Absorption coefficient

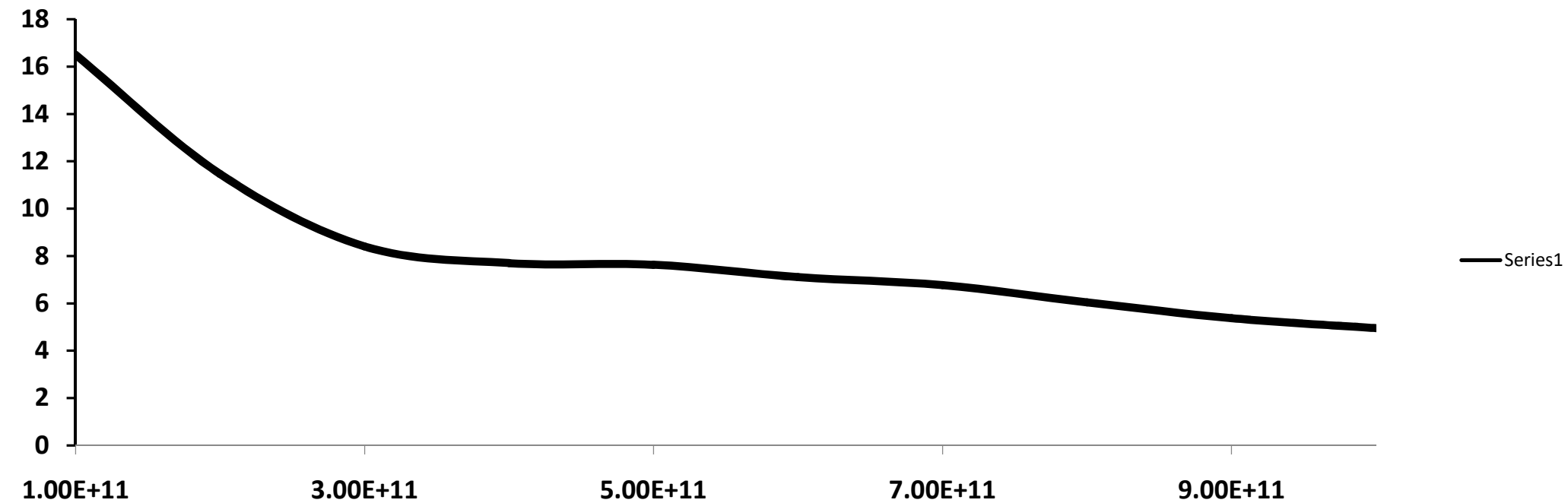
\*Blank Circles are Experimental Results, Solid line simulated



# Ge Characteristics: @10 kV/cm @ 294K



Conductivity [S/m] w.r.t THz at 10 kV/cm

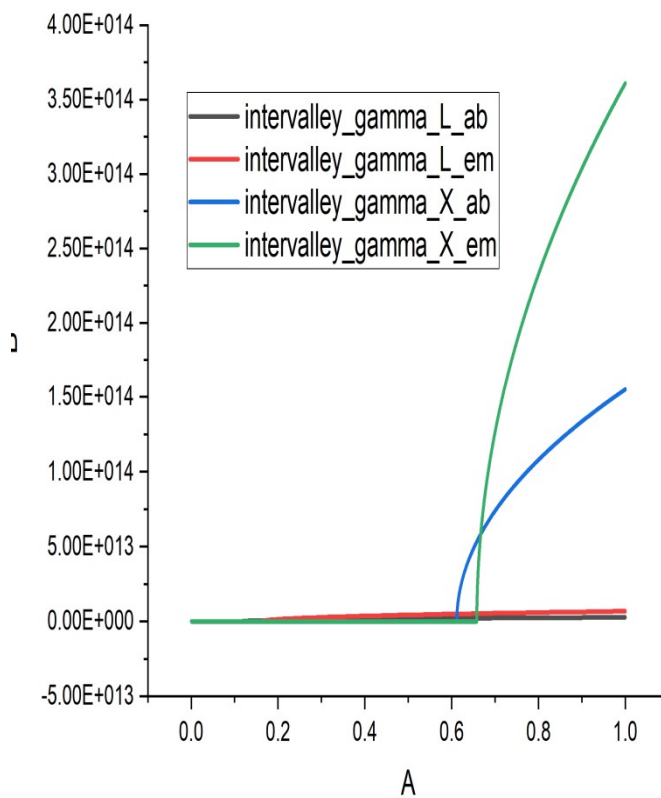


# Ge Characteristics: @10 kV/cm @ 294K

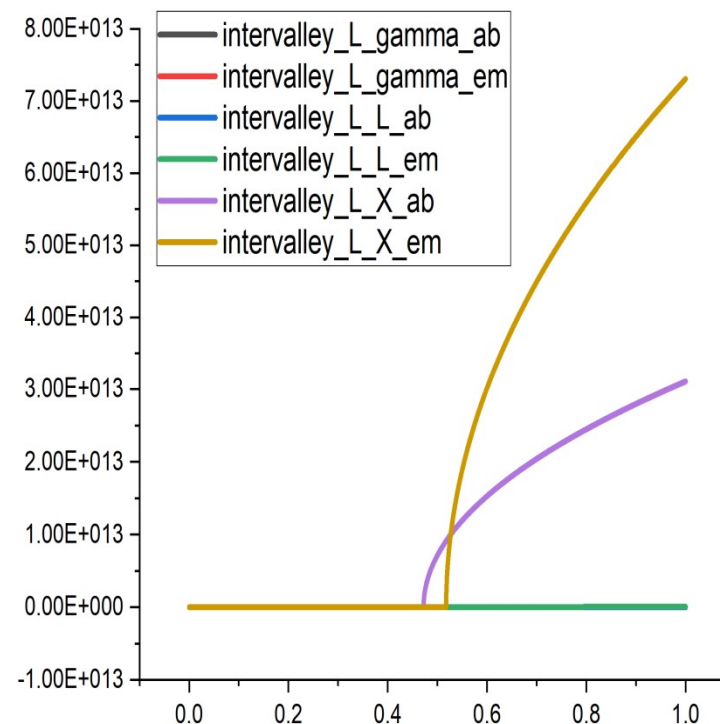


## Scattering Rates ( $s^{-1}$ ) w.r.t Energy (eV)

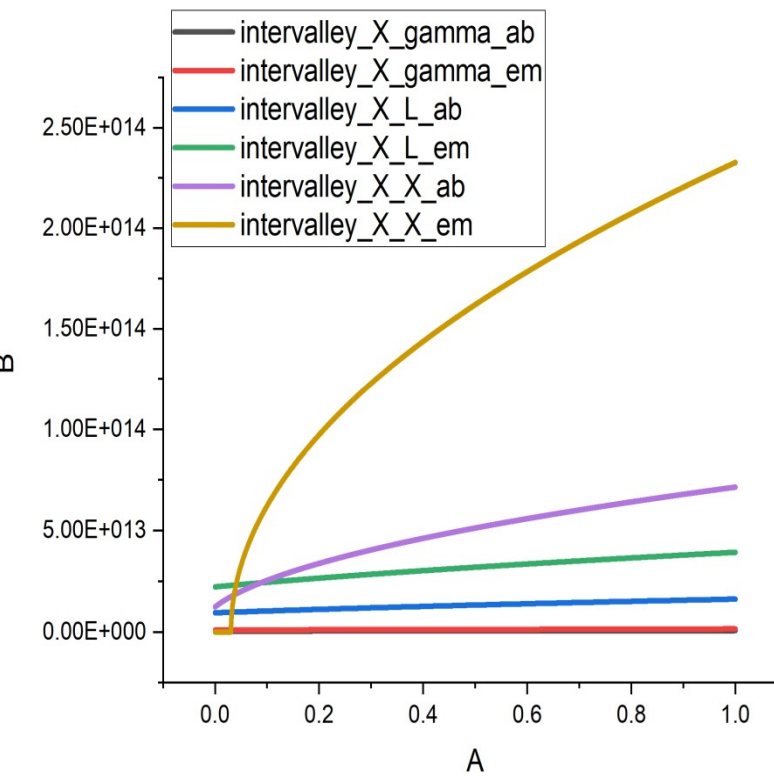
## **Γ - Valley**



L - Valley



X - Valley



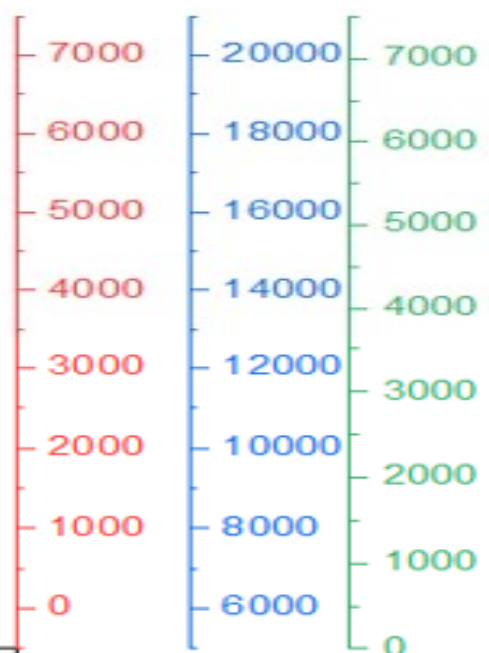
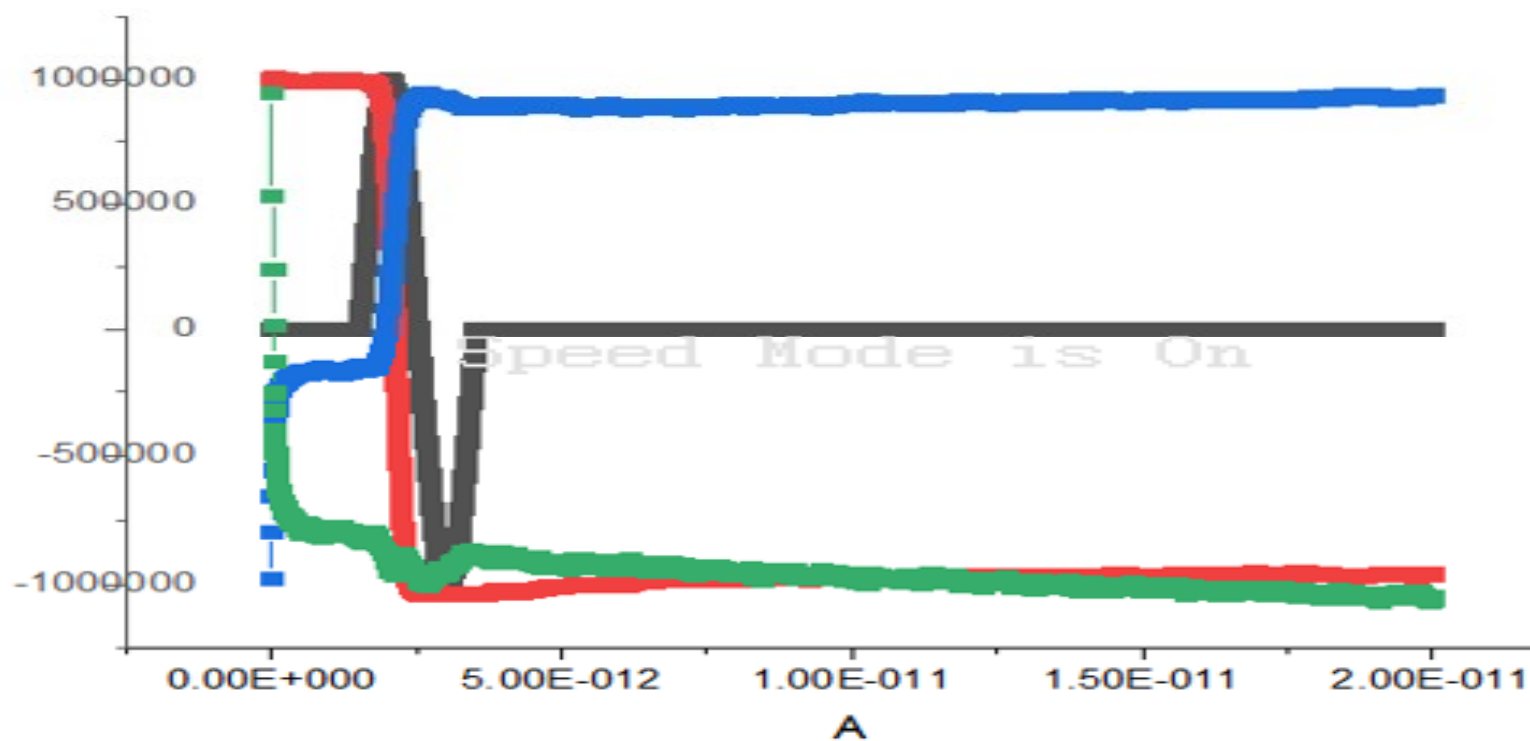
# CARRIER TRANSITIONS



ONLY Intervalley Scattering mechanism at 10 kV/cm

1 2 3 4

—■— B  
—■— C  
—■— D  
—■— E



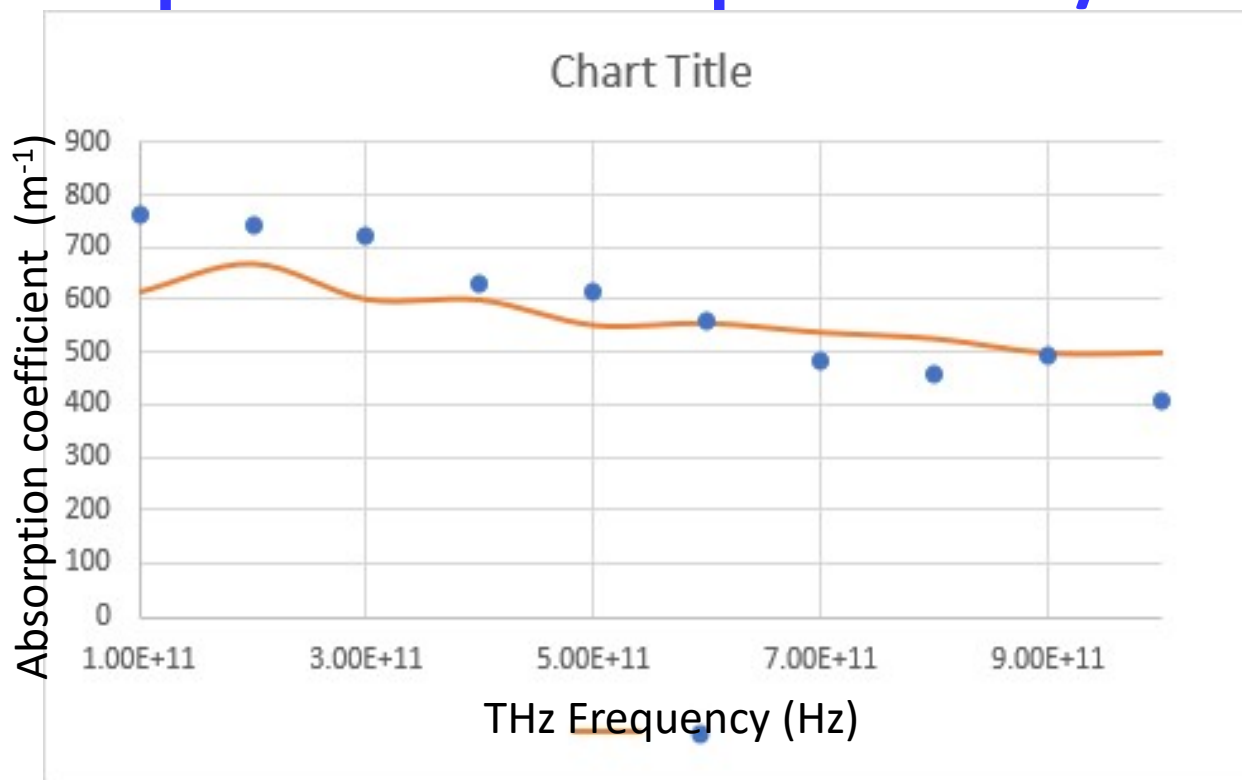
# Ge Characteristics: @181 kV/cm @ 294K



## Absorption ( $\text{m}^{-1}$ ) with respect to THz Freq at 181 kV/cm

- Material: Ge “n doped”
- Temperature: 294 K
- Different THz fields
- Absorption coefficient

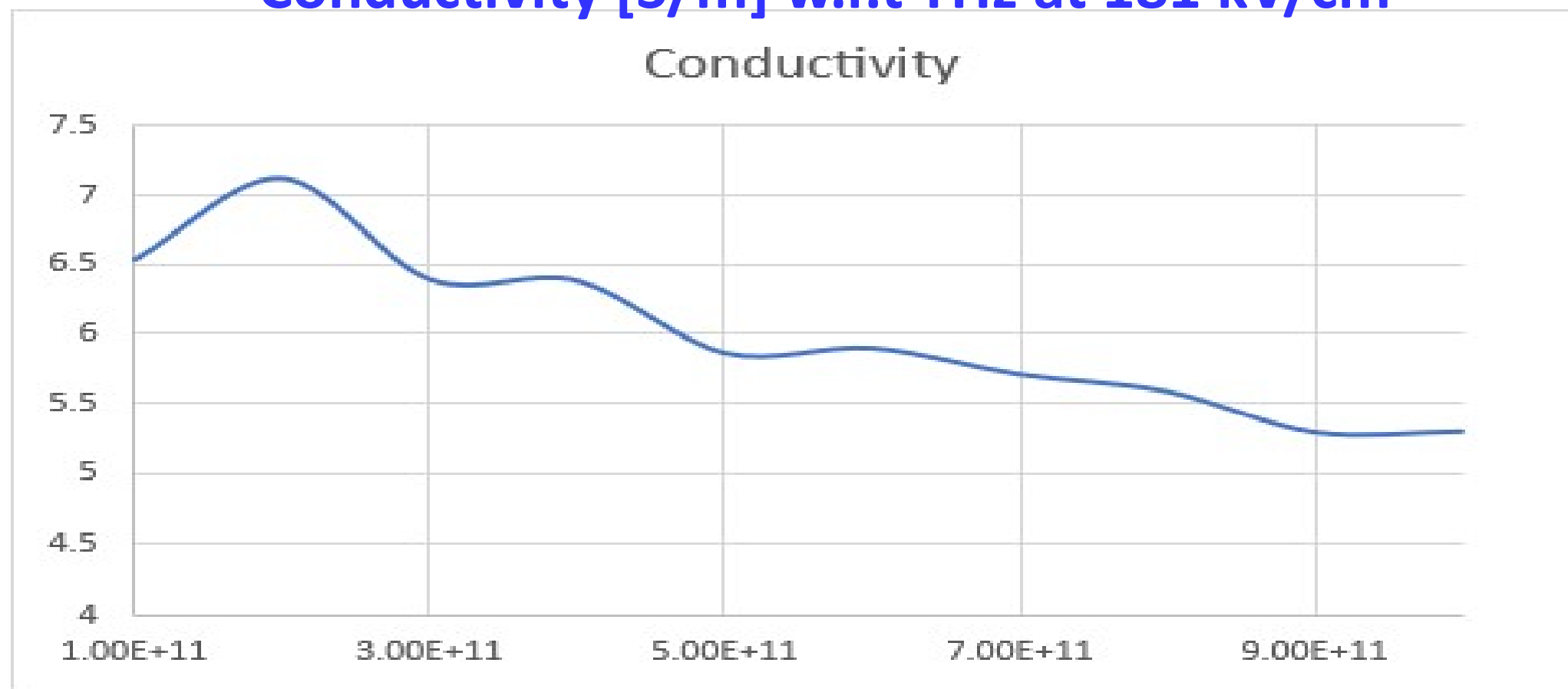
\*Circles are Experimental Results, Solid line simulated



# Ge Characteristics: @181 kV/cm @ 294K



Conductivity [S/m] w.r.t THz at 181 kV/cm

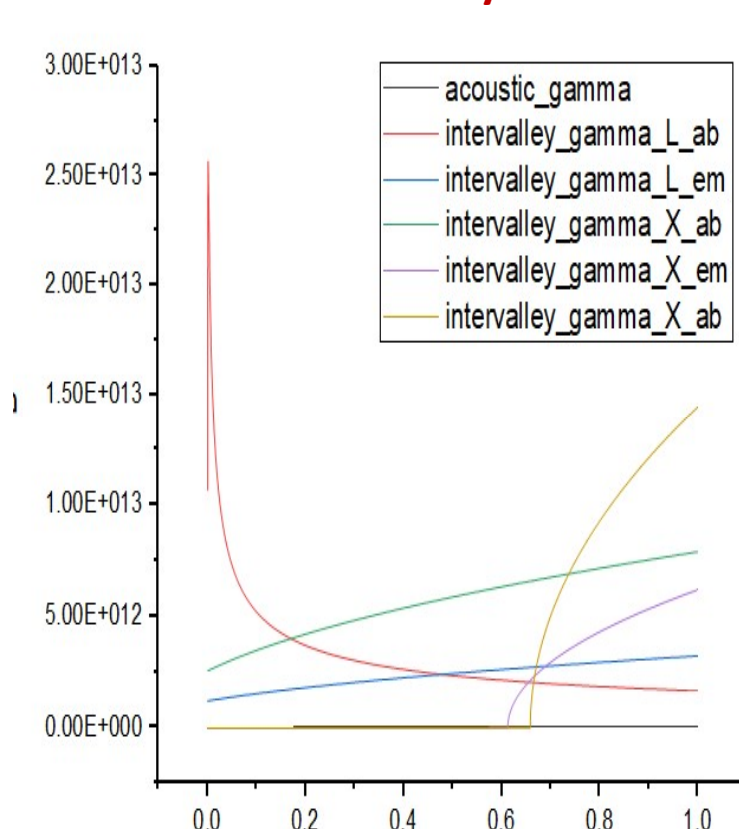


# Ge Characteristics: @181 kV/cm @ 294K

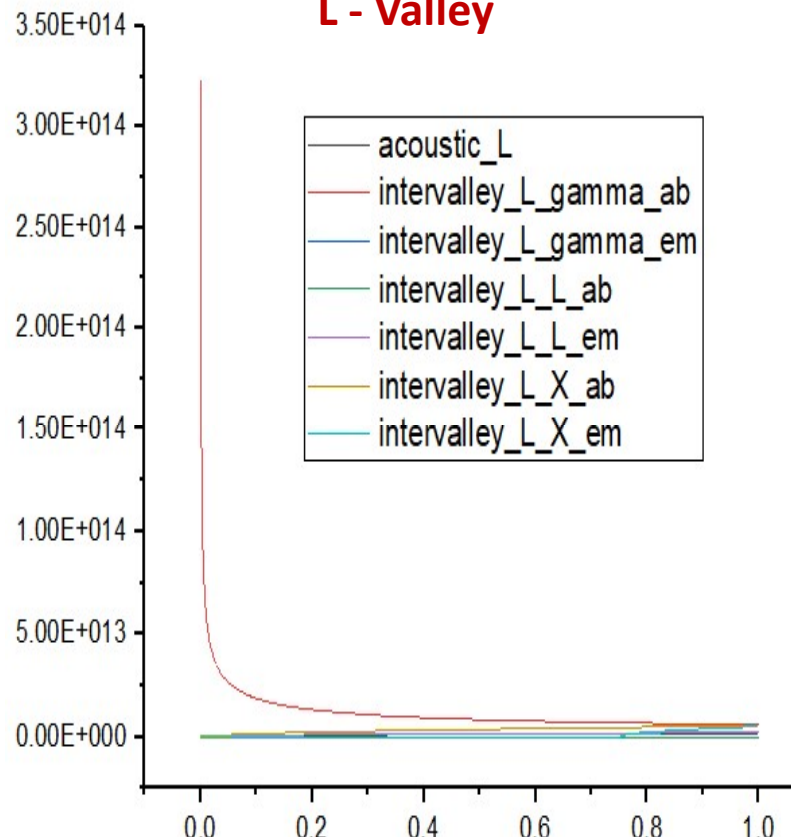


## Scattering Rates ( $s^{-1}$ ) w.r.t Energy (eV)

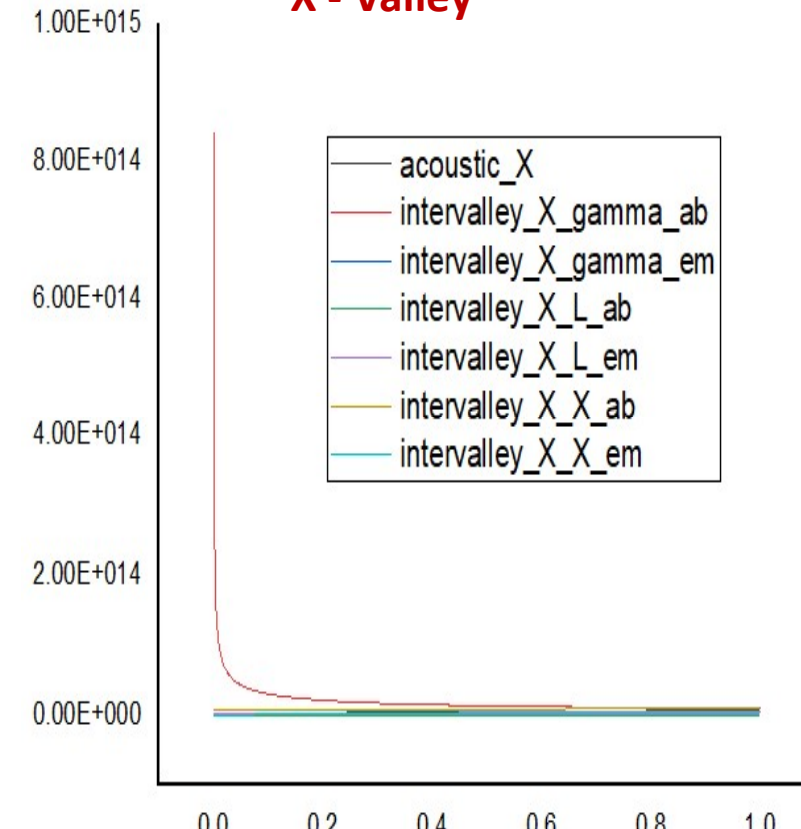
$\Gamma$  - Valley



L - Valley



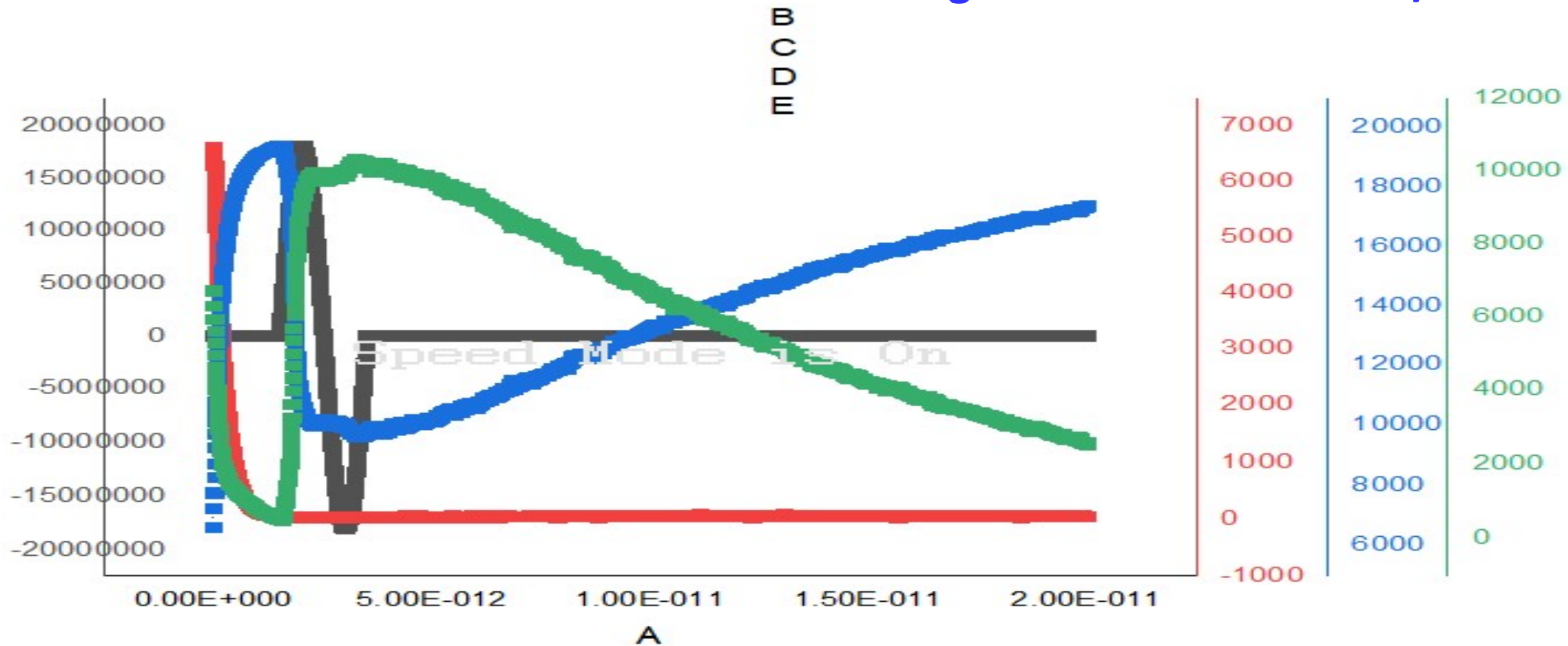
X - Valley



# Ge Characteristics: @181 kV/cm @ 294K



Carrier Transitions due to Scattering mechanism at 181 kV/cm

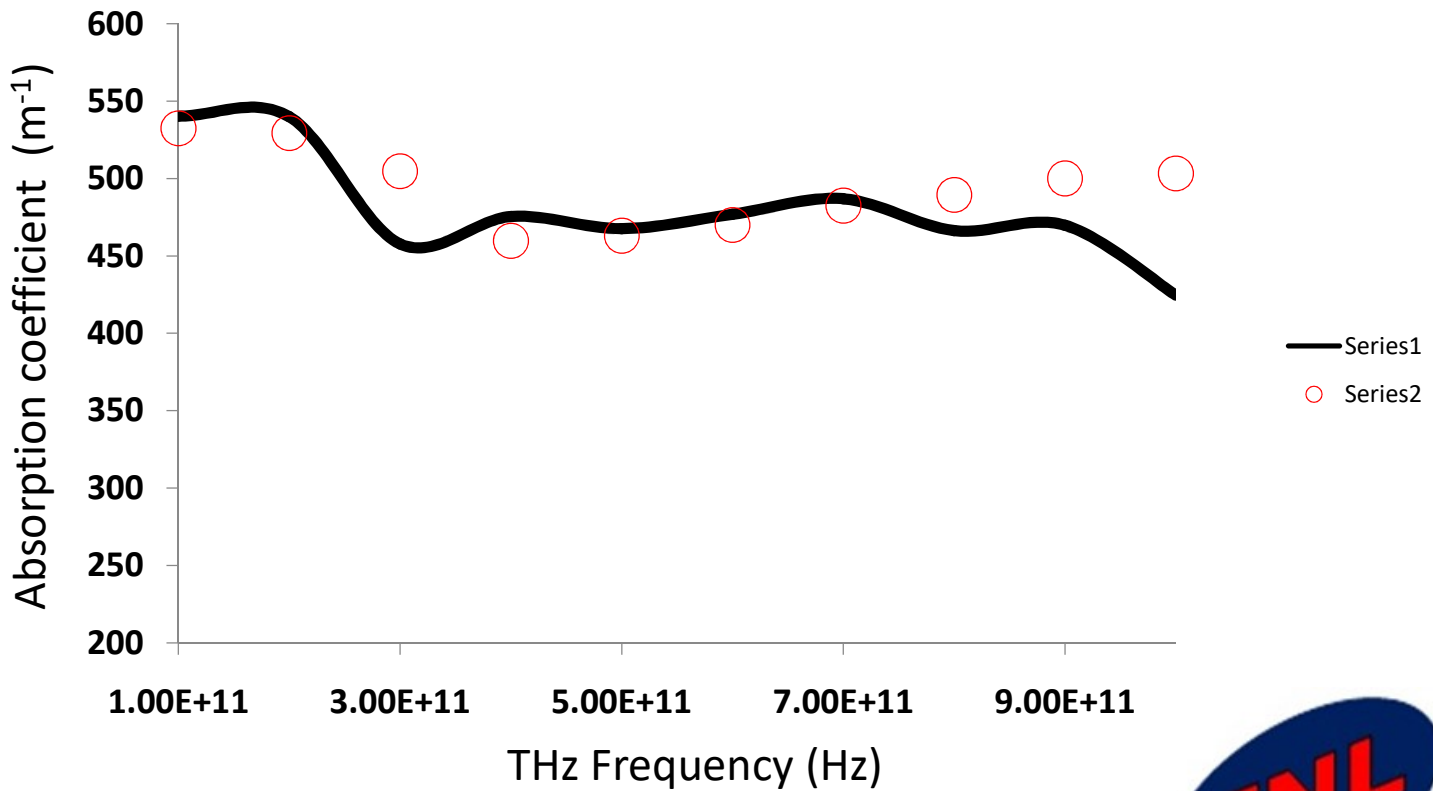


# Ge Characteristics: @441 kV/cm @ 294K



## Absorption ( $\text{m}^{-1}$ ) with respect to THz Freq at 441 kV/cm

- Material: Ge “n doped”
- Temperature: 294 K
- Different THz fields
- Absorption coefficient



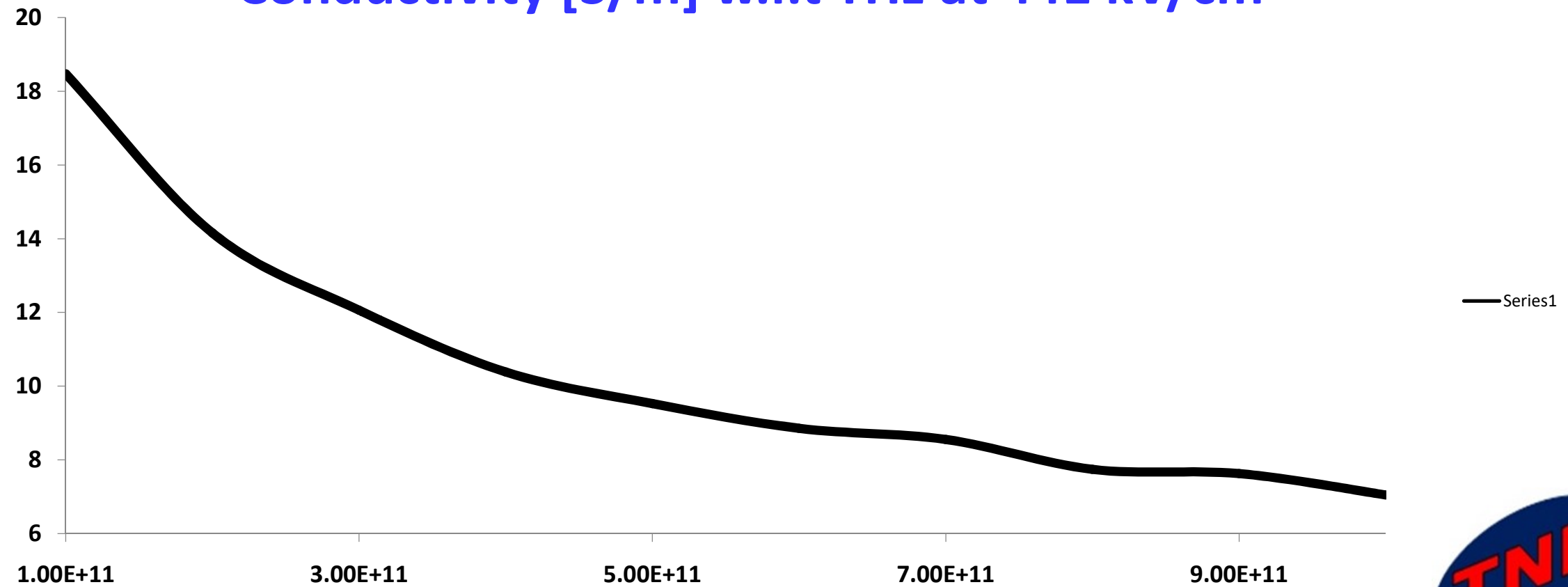
\*Circles are Experimental Results, Solid line simulated



# Ge Characteristics: @441 kV/cm @ 294K



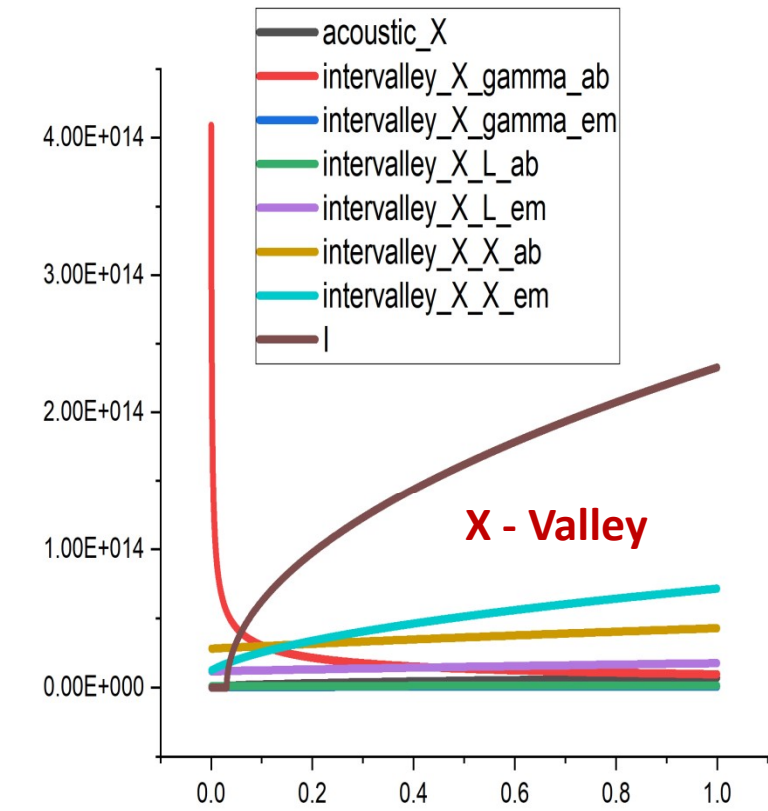
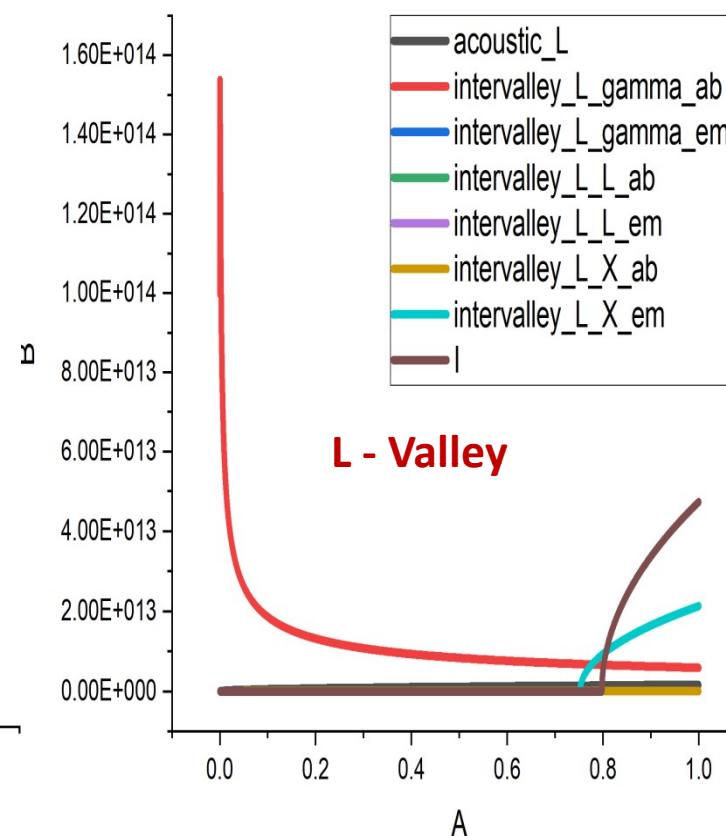
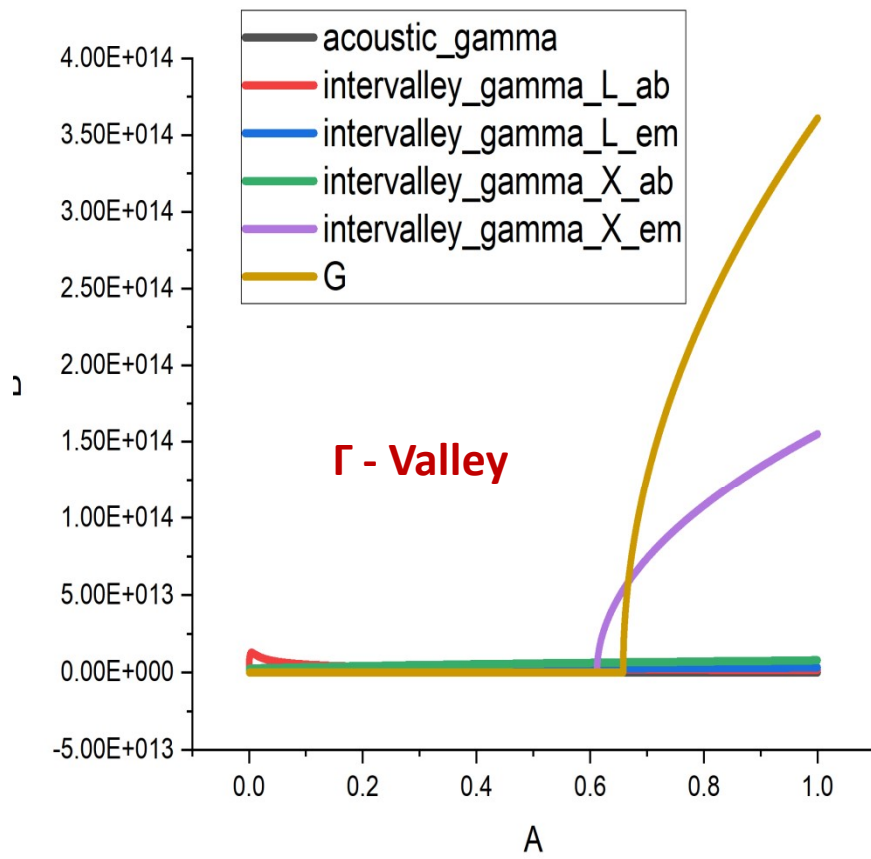
Conductivity [S/m] w.r.t THz at 441 kV/cm



# Ge Characteristics: @441 kV/cm @ 294K



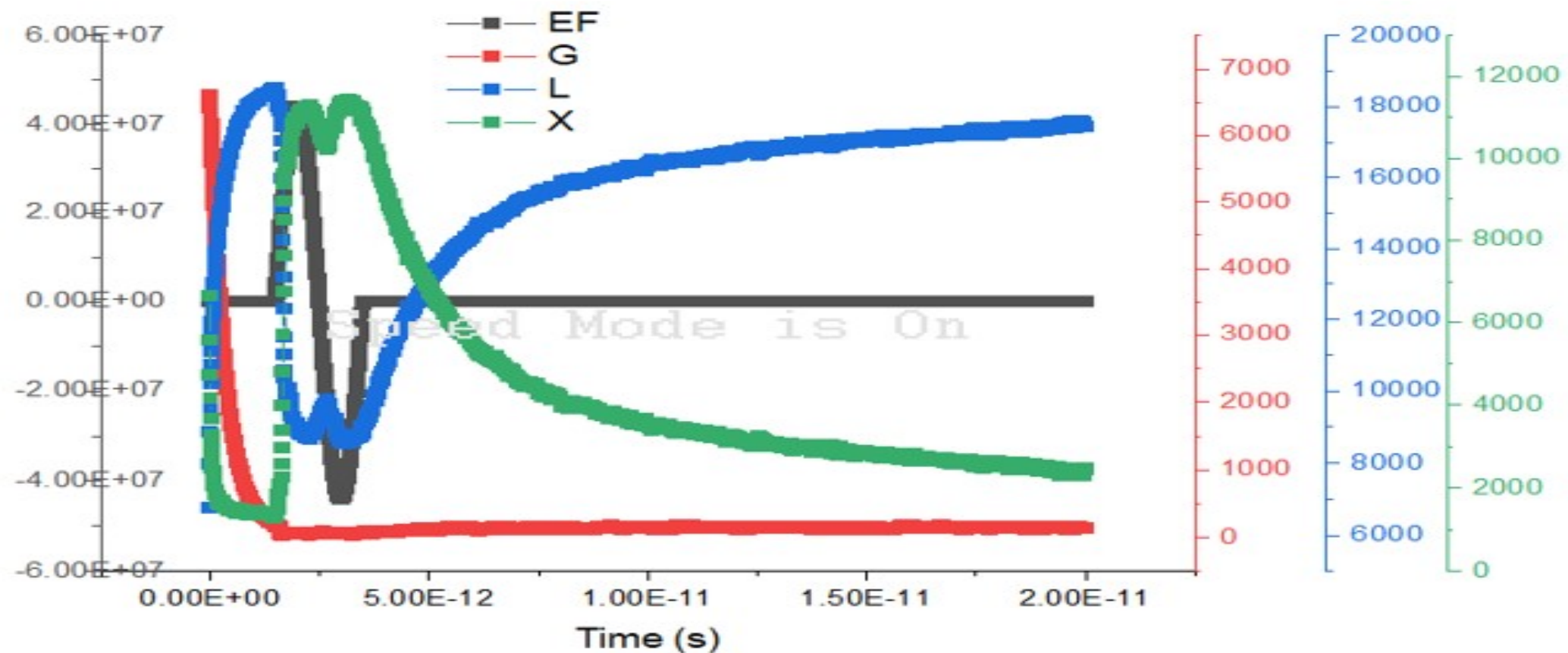
## Scattering Rates ( $s^{-1}$ ) w.r.t Energy (eV)



# Carrier Transitions



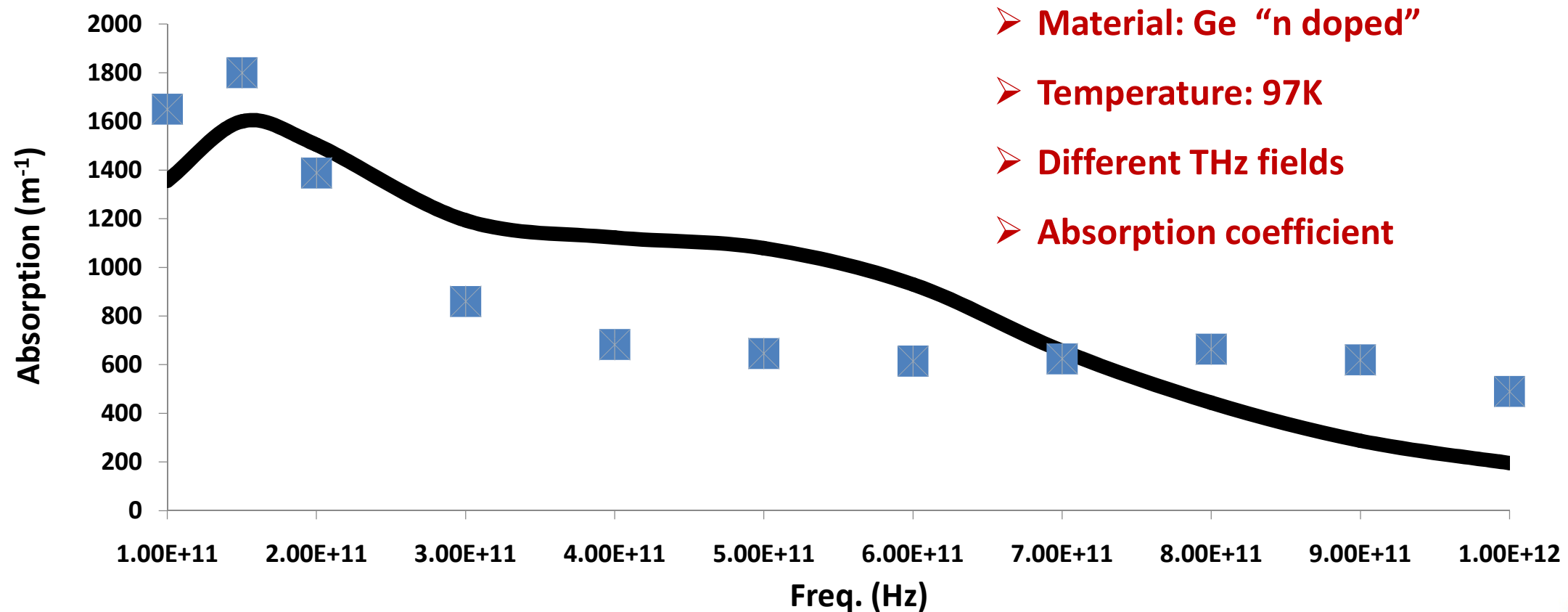
Carrier Transitions due to Scattering mechanism at 441 kV/cm



# Ge Characteristics: @10 kV/cm @ CT



## Absorption ( $\text{m}^{-1}$ ) with respect to THz Freq at 10 kV/cm



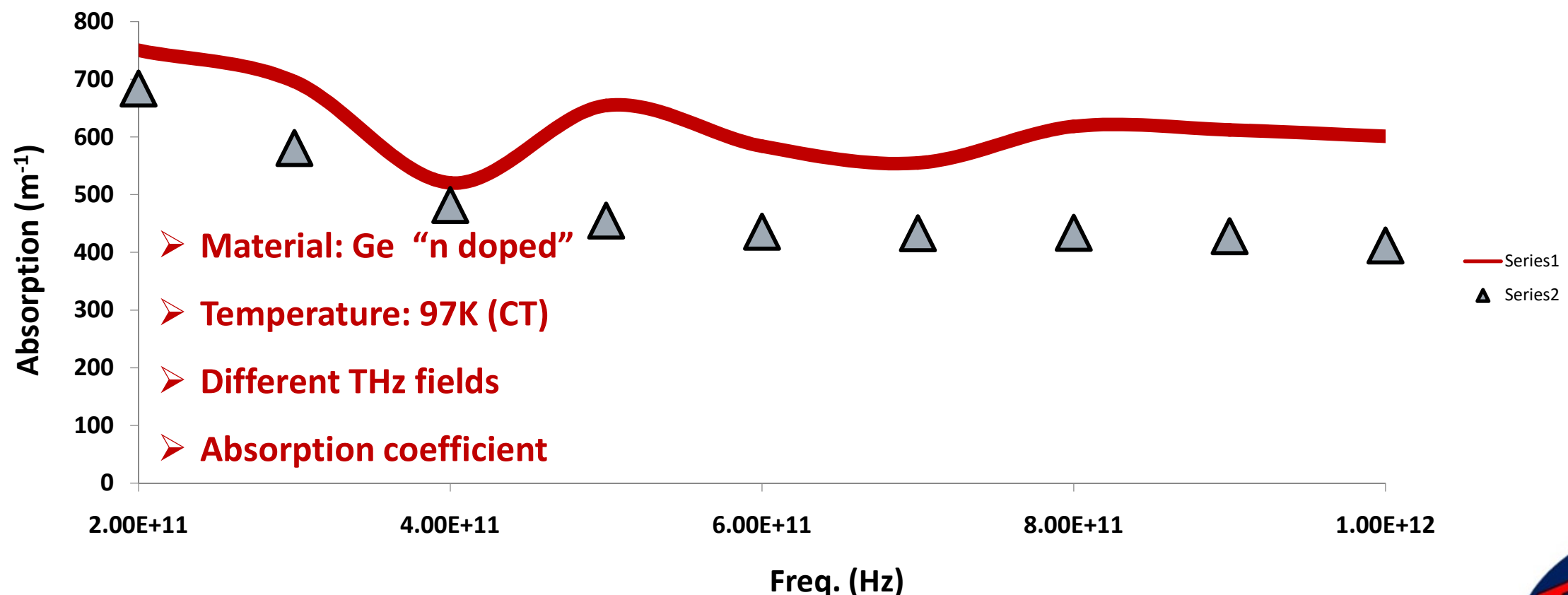
\*Circles are Experimental Results, Solid line simulated



# Ge Characteristics: @441 kV/cm @ CT



## Absorption ( $\text{m}^{-1}$ ) with respect to THz Freq at 441 kV/cm



\*Circles are Experimental Results, Solid line simulated



# GaAs Full Band Structure



## Symmetry points

At  $k=0$  showing L valley

$$L = \frac{2\pi}{a} \left( \frac{1}{2}, \frac{1}{2}, \frac{1}{2} \right)$$

At  $k=10$ , the curve shows the Gamma valley

$$\Gamma = \frac{2\pi}{a} (0, 0, 0)$$

At  $k=20$ , the curve shows the X valley

$$X = \frac{2\pi}{a} (1, 0, 0)$$

At  $k=25$ , the curve shows the W valley

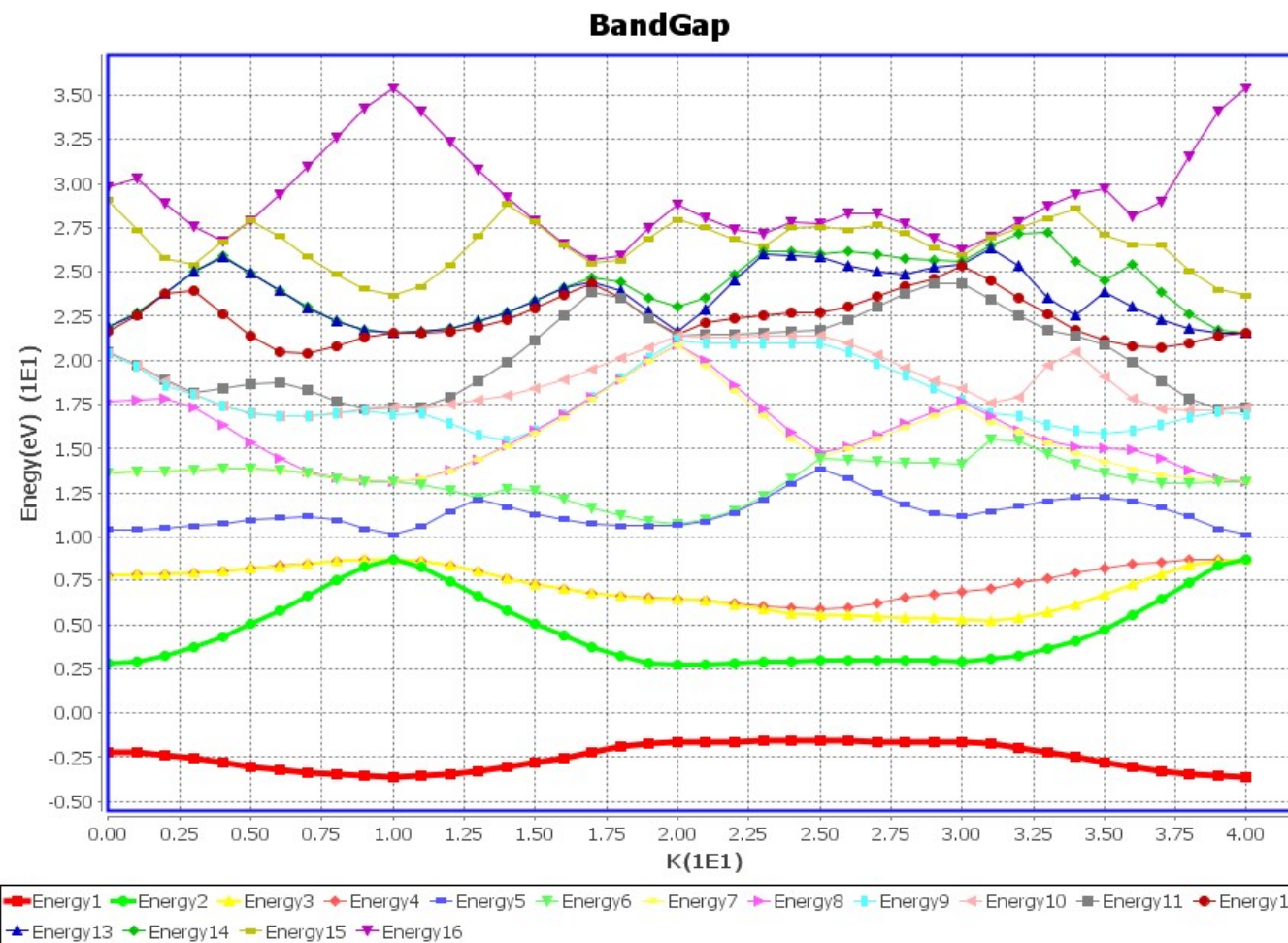
$$W = \frac{2\pi}{a} (1, \frac{1}{2}, 0)$$

At  $k=30$ , the curve shows the K valley

$$K = \frac{2\pi}{a} (\frac{3}{4}, \frac{3}{4}, 0)$$

At  $k=40$ , the curve again shows the Gamma valley

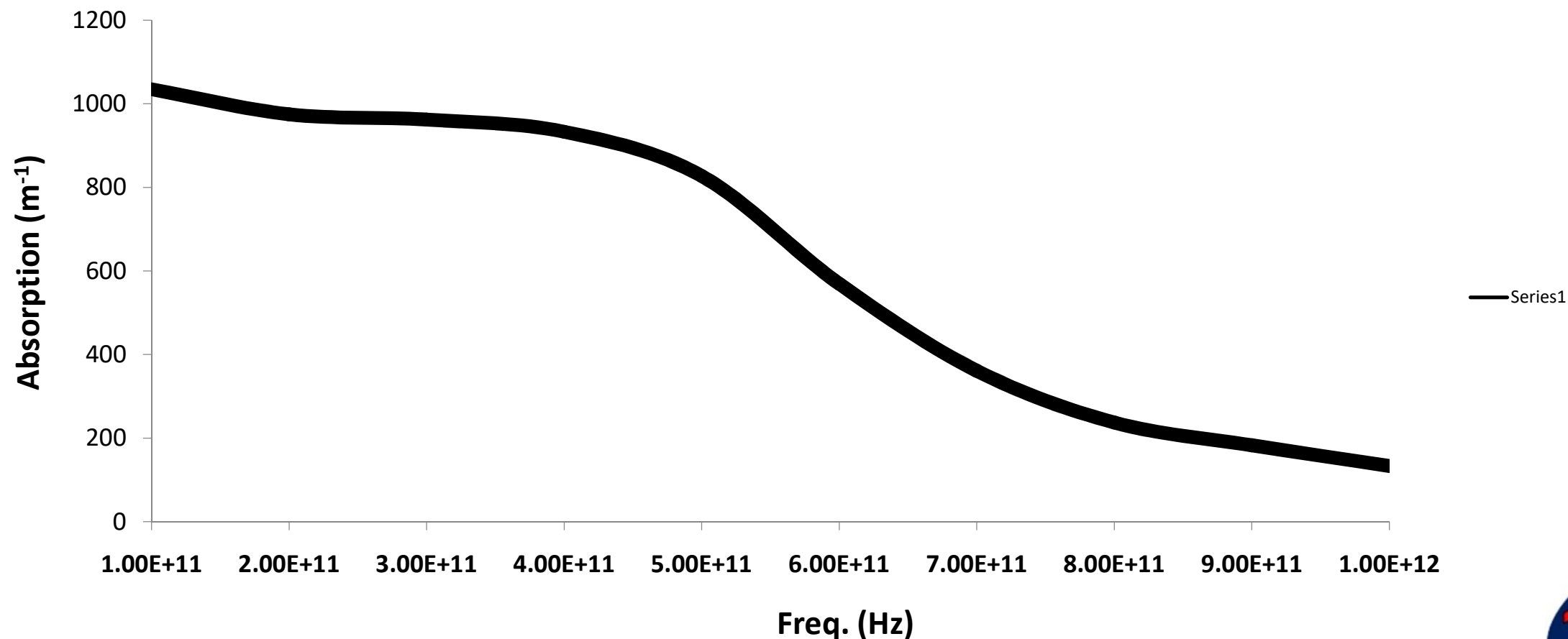
$$\Gamma = \frac{2\pi}{a} (0, 0, 0)$$



# GaAs Results



Absorption ( $\text{m}^{-1}$ ) with respect to THz Freq at 10 kV/cm



# Conclusion



- Successfully demonstrated the THz conductivity of a weakly confined Drude gas of electrons of Ge and GaAs at room and cryogenic temperatures.
- *TNL-TS simulator* predictions agree remarkably well with experimental data without any assuming any fitting parameters artificially.
- The amount of absorbed THz energy and the number of carriers in the illuminated volume indicates that the average energy deposited per free carrier at the highest pump pulse intensity was recorded 2.1 eV in GaAs and 0.9 eV in Ge.
- Providing access to side valleys at higher energies: the L (0.31 eV) and X (0.52 eV) valleys in GaAs and the  $\Gamma$  (0.14 eV) and X (0.19 eV) valleys in Ge.
- The energized electrons scattered into the side valleys during the THz pump pulse because the intervalley scattering time is typically on the sub-picosecond time scale.
- Since the mobility in the X valley of Ge is nearly five times smaller than in the initial L valley, scattering into the X valley decreases the free-carrier absorption .



# Publications



1. P.K. Saxena, numerical study of dual band (MW/LW) ir detector for Performance improvement, *Defence Science Journal*, vol. 67(2), (2017) pp. 141-148. DOI : 10.14429/dsj.67.11177
2. Praveen K. Saxena, Pankaj Srivastava, R. Trigunayat, An innovative approach for controlled epitaxial growth of GaAs in real MOCVD reactor environment, *Journal of Alloys and Compounds*, vol. 809 (2019) 151752.  
<https://doi.org/10.1016/j.jallcom.2019.151752>
3. Praveen Saxena, R. Trigunayat, Anchal Srivastava, Pankaj Srivastava, Md. Zain, R.K. Shukla, Nishant Kumar, Shivendra Tripathi, FULL ELECTRONIC BAND STURCTURE ANALYSIS OF Cd DOPED ZnO THIN FILMS DEPOSITED BY SOL-GEL SPIN COATING METHOD , II-VI US Workshop Proceedings, 2019.
4. R. K. Nanda, E. Mohapatra, T. P. Dash, P. Saxena, P. Srivastava, R. Trigutnayat, C. K. Maiti, Atomistic Level Process to Device Simulation of GaNFET Using TNL TCAD Tools, [Advances in Electrical Control and Signal Systems](#) pp 815-826, (2020), Spinger Book. [https://doi.org/10.1007/978-981-15-5262-5\\_61](https://doi.org/10.1007/978-981-15-5262-5_61)
5. Sanjeev Tyagi, P. K. Saxena, Rishabh Kumar, Numerical simulation of  $In_xGa_{1-x}As/InP$  PIN photodetector for optimum performance at 298 K, *Optical and Quantum Electronics* (2020) 52:374.  
<https://doi.org/10.1007/s11082-020-02488-1>
6. Many Mores



**Thank You**  
Contact us



+91-983-915-1284



[info@technextlab.com](mailto:info@technextlab.com)



Lucknow 226 003, INDIA



[www.technextlab.com](http://www.technextlab.com)

